



UNIVERSITY OF CORDOBA
INSTITUTE OF POSTGRADUATE STUDIES



UNIVERSITY MASTER'S DEGREE

**PHYSICAL TECHNOLOGY:
RESEARCH AND APPLICATIONS**

MASTER'S THESIS

**Exploring the relationship between Hawkes processes
and self-organized criticality in living systems**

Antonio Rivas Blanco

Tutor(s): Jorge Hidalgo Aguilera and Serena di Santo

Line of research: Modelling of complex systems and their interdisciplinary applications

Córdoba, 07/2024

Autorización de defensa del Trabajo Fin de Máster

Tutor 1: Jorge Hidalgo Aguilera

Tutor 2: Serena di Santo

INFORMAN: Que el presente trabajo titulado *Exploring the relationship between Hawkes processes and self-organized criticality in living systems* que constituye la memoria del Trabajo Fin de Máster ha sido realizado por Antonio Rivas Blanco y AUTORIZA/N su presentación para que pueda ser defendido en la convocatoria 1ª con fecha 23/07/2024.

Firmado en Córdoba a X de julio de 2024

Tutor 1: Jorge Hidalgo Aguilera

Tutor 2: Serena di Santo

Declaración de autoría

Nombre y apellidos: Antonio Rivas Blanco
DNI: 49832223D

DECLARA

1. Que el trabajo que presenta es totalmente original y que se hace responsable de todo su contenido.
2. Que no ha sido publicado ni total ni parcialmente.
3. Que todos los aportes de otros autores/as han sido debidamente referenciados.
4. Que no ha incurrido en fraude científico, plagio o vicios de autoría.
5. Que, en caso de no cumplir los requerimientos anteriores, aceptará las medidas disciplinarias sancionadoras que correspondan.

Firmado en Córdoba a, X de julio de 2024

Contents

Contents	III
List of Figures	IV
List of Tables	VI
Abstract. Keywords	1
1 Introduction	2
1.1 Criticality and its presence in living systems	2
1.2 Point processes	4
1.2.1 Poisson processes	5
1.2.2 Hawkes processes	6
2 Objectives	12
3 Methodology	13
3.1 Time series factory	13
3.2 When physics and cooking merge	17
4 Results	20
4.1 Results from the original paper	20
4.2 Results for $n=2$	23
4.3 Inhibitory and excitatory neurons coupled	26
5 Conclusions	30
A Python scripts	33

List of Figures

1.1	On the left, the dynamics of the SIS model, which is a typical contact process for disease spreading. On the right, the order parameter versus the control parameter; In this case, the control parameter would be the infection rate λ . The order parameter is the fraction of infected individuals. Here we would have a critical point at $\lambda = \lambda_c = \mu$	3
1.2	On the left, a subcritical branching process, in the middle, a critical branching process and on the right, a supercritical branching process. Each color represents a different generation.	3
1.3	On the left, a subcritical percolation process, on the right, a critical percolation process. The blue line represent the percolant cluster.	4
1.4	Representation of a point process. The intensity function $\lambda(t)$ is a time-dependent function.	5
1.5	Left: event number in time for different rates. Right: Probability of having a certain number of events for different rates.	6
1.6	On the left, a temporal series of $K = 150$ events of a Hawkes process with $\mu = 0.01$, on the right, a raster plot of the same process.	7
1.7	On the left, a temporal series of $K = 150$ events of a Hawkes process with $\mu = 0.01$, on the right, a raster plot of the same process.	7
1.8	First, a temporal series of $K = 10^5$ events of a Hawkes process with $\mu = 0.01$, on the right, the event distribution.	8
1.9	First, a temporal series of $K = 10^5$ events of a Hawkes process with $\mu = 10$, on the right, the event distribution.	8
1.10	On the left, a temporal series of $K = 10^5$ events of a Hawkes process with $\mu \in \{10^{-2}, 10^2\}$ and $n = 2$, on the right, the λ distribution versus the event number.	9
1.11	Raster plots of Hawkes processes with $n = 2$. In both cases, the number of events is $K = 10^3$, they also have the same structure, the first event, on average, happens in $\mu^{-1}a.u.$ of time; then, an avalanche of events takes place.	9
1.12	Scheme of the interaction between the excitatory and inhibitory populations. As illustrated, the excitatory population can excite itself and the inhibitory population, while the inhibitory population can only inhibit the excitatory population, because on most cases the auto-inhibition is negligible [17].	10
1.13	On the left, a temporal series of $K = 10^4$ events of a bivariate Hawkes process with the interaction parameters of the pseudo-critical signal shown in Table 1.1, on the right, the raster plot of the same process for excitatory and inhibitory events.	11
1.14	On the left, a temporal series of $K = 10^4$ events of a bivariate Hawkes process with the interaction parameters of the “stable” signal shown in Table 1.1, on the right, the raster plot of the same process for excitatory and inhibitory events.	11
3.1	Diagram to calculate the cumulative probability of the inter-event time.	14

3.2	Five a temporal series of $K = 10^5$ events of Hawkes processes with $\mu = 10^{-4}$ on the left side and $\mu = 10^2$ on the right one.	18
3.3	Diagram for $\mu \ll 1$. Red lines represent the events, clusters are coloured. As we can see, we have two regimes, one when Δ is of the order of the average cluster size and another when is of the order of the inter-event time where the system percolates. . . .	19
3.4	Diagram for $\mu \gg 1$. Red lines represent the events, clusters are coloured. In this situation, events occur more regularly, resulting in a unique transition corresponding the case of Δ is similar to the inter-event time producing the system percolation. . . .	19
4.1	Percolation phase diagrams for different event number K taking average values of $R = 1000$ realizations.	20
4.2	Susceptibility χ normalized to the number of evetns K , for different event number K and taking average values for $R = 1000$ realizations.	21
4.3	Avalanche analysis for Hawkes process with $n = 1$, $K = 10^5$ events. The histograms have been calculated over $R = 1000$ time series.	22
4.4	At the left, the vertical dashed lines represent the critical points $\Delta^*(K)$ for the Poisson process. At the right, the vertical dashed lines represent the critical points $\Delta_1^*(K)$ given by Eq. 4.2 and the dotted dashed lines the $\Delta_1^*/100$	23
4.5	Event series for $n = 1$ and $n = 2$	23
4.6	Percolation phase diagrams for a Hawkes process with $n = 2$	24
4.7	Susceptibility χ normalized to the number of evetns K , for different event number K and taking average values for $R = 1000$ realizations.	24
4.8	Avalanche statistics for a self-exciting Hawkes process with $n = 2$ for $K = 10^5$ events. The histograms have been calculated over $R = 1000$ time series.	25
4.9	Percolation phase diagrams averaged over $R = 1000$ “pseudo-critical” signals of $K = 10^5$ events.	26
4.10	Susceptibility χ normalized to the number of events associated with the above the phase diagram.	26
4.11	Avalanche statistics of $K = 10^5$ events for “pseudo-critical” signals of two coupled Hawkes processes. Histograms have been calculated over $R = 1000$ time series.	27
4.12	Percolation phase diagrams averaged over $R = 1000$ “controlled” signals of $K = 10^5$ events.	27
4.13	Susceptibility χ normalized to K associated with the above the phase diagram.	28
4.14	Avalanche statistics of $K = 10^5$ events for “controlled” signals of two coupled Hawkes processes. Histograms have been calculated over $R = 1000$ time series.	28

List of Tables

1.1	Interaction parameters for both bivariate processes	10
3.1	Configuration of the parameters for the simulations of the article [9]	17
4.1	Power-law exponents for every configuration studied.	29

List of Algorithms

1	Slow method to generate Hawkes processes.	13
2	Algorithm to generate K Hawkes events.	16
3	Algorithm to generate K Hawkes events for two coupled processes.	17

Abstract

Chapter 1

Introduction

The following Master's thesis is divided into five chapters. In the first chapter, we will introduce the concept of criticality in complex systems, both in living and non-living systems. We will also make a brief summary of stochastic and their relation with point processes and Hawkes processes, which are the main focus of this work. After that, we will present the objectives of this work. In the third chapter, we will present the methodology used in this work, including the simulation of Hawkes processes, the phase diagram of the process, and the avalanche analysis. In the penultimate chapter, we will present the results of the simulations, including the phase diagram of the process, the susceptibility analysis, and the avalanche analysis and we will discuss them. Finally, in the fifth chapter, we will present the conclusions of this work and the future lines of research.

1.1 Criticality and its presence in living systems

Criticality is one of the key concepts around complex systems because it is believed that they are benefited by working in a critical state or near it. It has been demonstrated that these states provide the system better properties such as robustness, adaptability, information processing and wider dynamic range thanks to the scale-invariance associated with the critical states [1]. This scale-invariance arises from a specific probability distribution, named Pareto or power-law distribution like $P(t) = Ct^{-\gamma}$. Where $\gamma \in \text{Re}^+$ and C is a normalization constant. In our case, we will focus on power-law distributions for avalanches of activity, the exponents for these distributions will be called α and τ for the size and duration of the avalanches respectively. It can be shown that they are the unique probability distribution that are free of scale. These distributions are present in many systems, such as earthquakes [2], epidemics [3] or social interactions [4, 5]. Although it is true that there are other mechanisms that can lead to power-law distributions, such as preferential attachment [6], we will focus on criticality.

The first time criticality was discussed was with Ising model [7], where it was shown that the model has a phase transition at a critical temperature T_c . This phase transition separated the system into two phases, an ordered phase where magnet's spins are aligned and when the temperature lower than the critical temperature, and a disordered phase being by thermal fluctuations when $T > T_c$. Ising model is an example of criticality in a system in equilibrium, but these phenomena are also present in systems out of equilibrium. Some the most studied systems in this context are the ones governed by contact processes due to their simplicity although they are able to show this kind of behaviour.

An example of these systems are the ones governed by contact processes, which are simple models that can show critical behaviour. These models' dynamics are based on the state of the system's constituents, which can be active or inactive and they can change their state interacting between them with a certain rate. For instance, an active site can activate an inactive site with a rate λ which

will be our control parameter and the inactive site can deactivate with a rate μ . These rates will be the key to understand the system's behaviour. In order to distinguish we need to define the order parameter, which is a quantity that allow us to stablish the phase [8]. An example is shown in Figure 1.1.

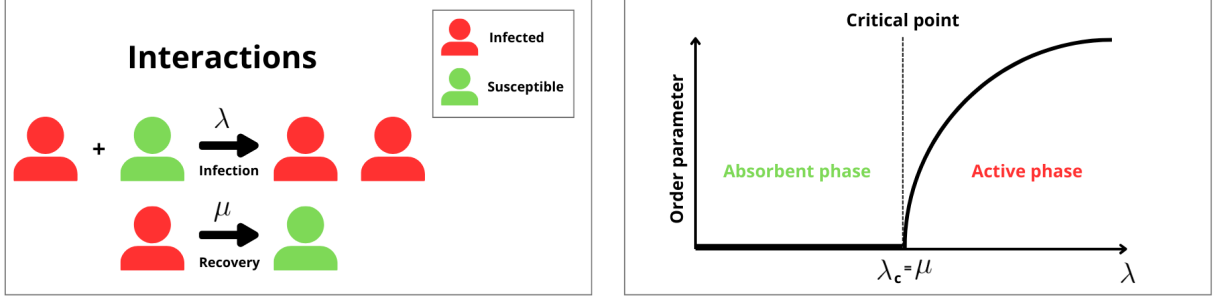


Figure 1.1. On the left, the dynamics of the SIS model, which is a typical contact process for disease spreading. On the right, the order parameter versus the control parameter; In this case, the control parameter would be the infection rate λ . The order parameter is the fraction of infected individuals. Here we would have a critical point at $\lambda = \lambda_c = \mu$.

Two other classic examples which are related with the results of this work are (critical) branching processes and percolation processes. The first one is used for example to model phenomena related with offspring. In a simplified way we can say that a parent can have a random number of children given by a probability distribution with a mean value n . We can discern between subcritical, critical and supercritical branching processes depending on this value. For the subcritical case, $n < 1$, and the process will die out eventually because the number of children will decrease with each generation. For the supercritical case, $n > 1$, the descendant population will grow exponentially. The most interesting situation is the critical case, $n = 1$, where we will have in average power law distributions for the tree size and the tree depth with exponents $\alpha \sim Z = 3/2$ and $\tau \sim D = 2$ respectively [9]. A representation of these situations is shown in Figure 1.2.

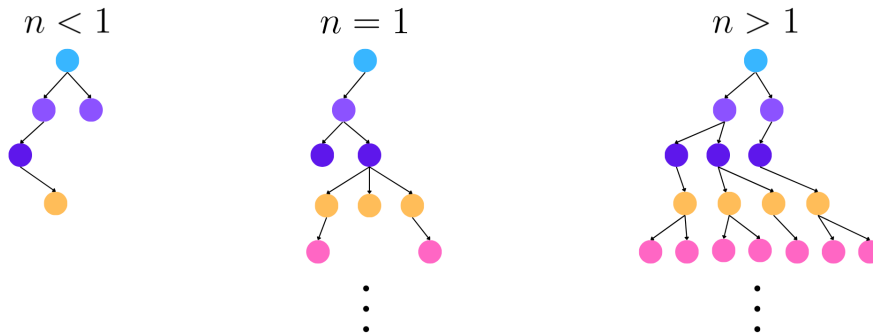


Figure 1.2. On the left, a subcritical branching process, in the middle, a critical branching process and on the right, a supercritical branching process. Each color represents a different generation.

To end up with the examples, we will finish with percolation. This processes are generally used to

model the flow of a fluid through a porous medium. Taking into account that this Master Thesis is related with living systems, there is not better example that relates the model with the topic and physics (indeed, physicist) than an Italian coffee maker. Here, the porous medium is coffee and the fluid is water. To describe the percolation process in a simple way, we can say that coffee makes a square lattice and the water will flow through the nodes with a certain probability p . We can define clusters of connected nodes (in this situation we are only interested on the vertical connections in order to make coffee) for a given probability, and we also define the order parameter as the size of the largest cluster. As same as the branching processes, we can discern between subcritical, and critical percolation processes depending on the value of p . For the subcritical case, $p < p_c$, the largest cluster will be smaller than the system size. In the same manner as the branching processes, the most interesting occasion is the critical case, $p = p_c$, where the largest cluster will be of the order of the system size, we will have at least a percolation cluster and we will have power law distributions. For our purposes, we will be interested in 1D percolation, whose exponents are $\alpha = 2$ and $\tau = 2$ [10]. A representation of these situations is shown in Figure 1.3.

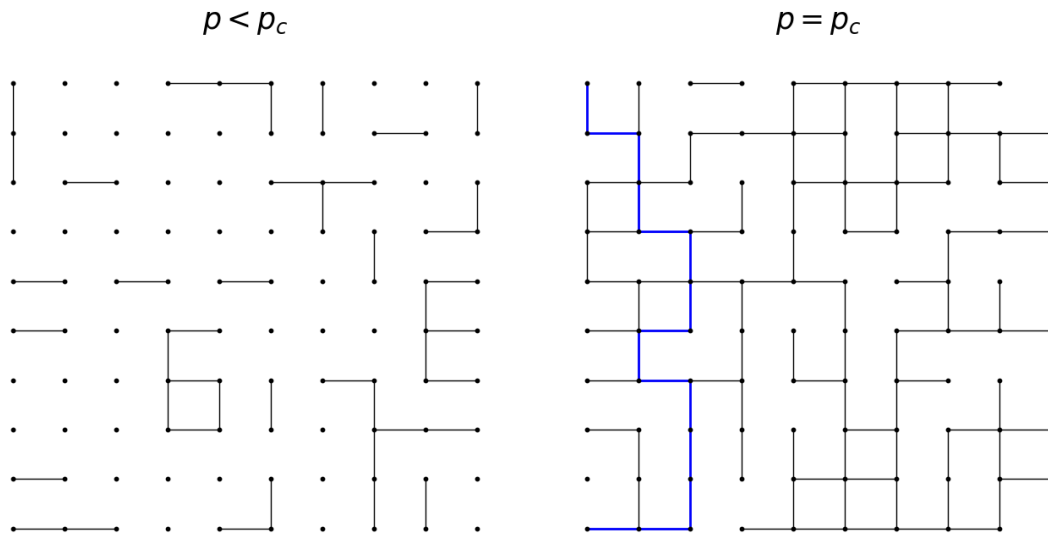


Figure 1.3. On the left, a subcritical percolation process, on the right, a critical percolation process. The blue line represent the percolant cluster.

Having seen these examples, we move on to a brief introduction to point processes which will lead us to another method to find criticality.

1.2 Point processes

Within the large framework of complex systems, stochastic processes lend us a hand to decypher properties of living systems, bridging randomness with structured behaviour. This processes are used to model the dynamics of systems which evolve randomly in time. This is why they are ideal for describing natural phenomena such as the spread of diseases [11], social networks [4] or ecological systems [12]. Mathematically, a stochastic process is a collection of random variables [13], generally ordered in time $\{X_t\}_{t \in T}$, where t is the time and X_t is the system state at time t . T is the time index set, which can be discrete or continuous, in this work we will focus on the discrete case because we

are interested in the study of point (Hawkes) processes for modeling neurons.

Point processes are a type of stochastic process that describe the occurrence of events in time or space. We will be interested in time point processes because we are going to model the spiking activity of neurons. For our purposes, they will be characterized by two parameters, the time of occurrence of the events t_k and the intensity or rate of occurrence of these events λ . This rate tell us how likely is that an event occurs at time t given the history of the process (probability density function, PDF) as pictured in Figure 1.4.

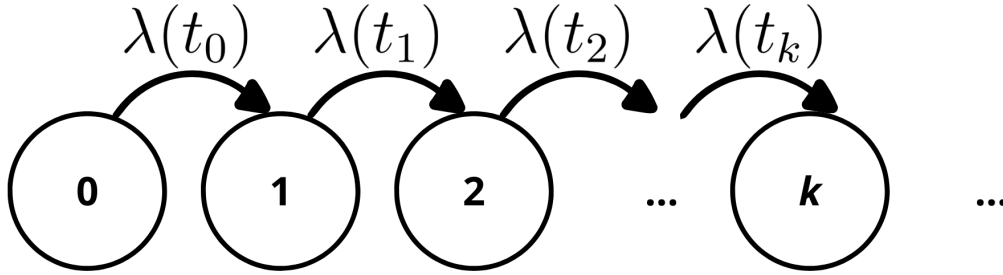


Figure 1.4. Representation of a point process. The intensity function $\lambda(t)$ is a time-dependent function.

1.2.1 Poisson processes

In general, the rate is a function of the history of the process, which makes the process non-Markovian, but in our case, it will be a Markovian process, which means that the rate depends only on the last event that occurred as we will see. An example of a Markovian point process is the Poisson process, which is a simple and one of the most studied point processes because they are present in many everyday situations such as the arrival of customers at a store, occurrence of defects on a Production line. They are also present in some physics phenomena, for instance, the decay of radioactive particles or the arrival of photons at a detector. These processes are characterized by a rate of occurrence of events λ . The dynamics of these processes are described by the Poisson distribution which is the probability distribution of a random variable N such that the probability that $N = n$ is:

$$P(N = n) = \frac{\lambda^n}{n!} e^{-\lambda}. \quad (1.1)$$

Furthermore, the mean value and the variance of the distribution are also equal to λ . Poisson processes can be homogeneous or inhomogeneous, depending on whether the rate is constant or time-dependent. In Figure 1.5 we can see an example of a homogeneous Poisson process.

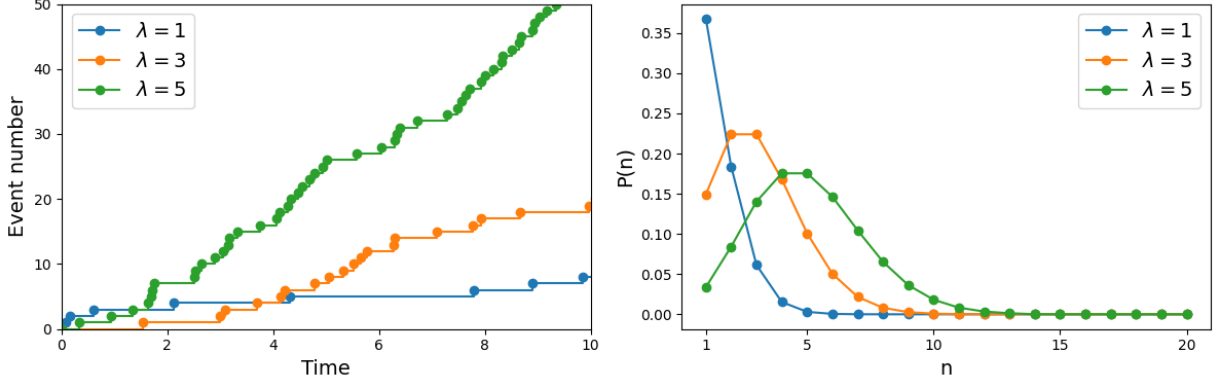


Figure 1.5. Left: event number in time for different rates. Right: Probability of having a certain number of events for different rates.

1.2.2 Hawkes processes

On the other hand if we consider a non-homogeneous Poisson process, the rate is a function of time, $\lambda(t)$, which is the case of the Hawkes process. The rate can be written in several ways [9, 14, 15, 16]. We will use the expression from [9]:

$$\lambda(t|t_1, \dots, t_k) = \mu + n \sum_{i=1}^k \phi(t - t_i), \quad (1.2)$$

where μ is the background rate of a homogeneous Poisson process, n is a parameter that controls the strength the self-excitation, and $\phi(t)$ is the kernel function that describes the influence of the past events on the rate of occurrence of the events. The kernel function is a non-negative and monotonically non-increasing function that integrates to 1. Typical choices for the kernel function are the exponential or the power-law functions. In this work we will focus on the exponential kernel. From Eq. 1.2 we can see that the rate depends on the history of the process, making it non-Markovian in general, but with an exponential kernel, the process becomes Markovian. The kernel function can be written as: $\phi(t) = \sum_{t_i < t} \alpha e^{-\beta(t-t_i)}$ so the rate becomes:

$$\begin{aligned} \lambda(t) &= \mu + \sum_{t_i < t} \alpha e^{-\beta(t-t_i)} \\ &= \mu + \sum_{\substack{t_i < t_k \\ t_k: \text{last event}}} \alpha e^{-\beta(t-t_k+t_k-t_i)} \\ &= \mu + e^{-\beta(t-t_k)} \underbrace{\sum_{t_i < t_k} \alpha e^{-\beta(t_k-t_i)}}_{\lambda(t_k)} \\ &= \mu + e^{-\beta(t-t_k)} (\lambda(t_k) - \mu + \alpha). \end{aligned} \quad (1.3)$$

Where we have used the following expression for the rate of the Hawkes process at time t_k :

$$\lambda(t_k) = \mu + \sum_{t_i < t_k} \alpha e^{-\beta(t_k - t_i)} \Rightarrow \sum_{t_i < t_k} \alpha e^{-\beta(t_k - t_i)} = \lambda(t_k) - \mu + \alpha \quad (1.4)$$

Despite being a Markovian process, it is still an inhomogeneous Poisson process because the rate is not constant. In addition, it is a self-exciting process, which means that the occurrence of an event increases the probability of the occurrence of another event. This is why it is used to model the spiking activity of neurons, where the occurrence of a spike increases the probability of the occurrence of another spike. This self-excitation will enable the appearance of bursts of activity that we will measure. The parameters chosen for the kernel function will be $\alpha = \beta = 1$ and we will vary the background rate μ from values much smaller than 1 to values greater than 1. In Figures 1.6 and 1.7 we can see typical diagrams of Hawkes processes with these parameters.

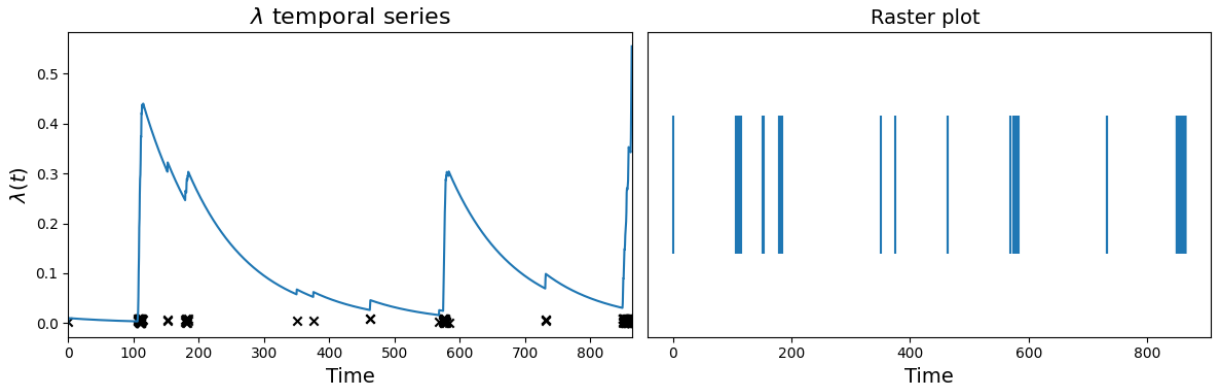


Figure 1.6. On the left, a temporal series of $K = 150$ events of a Hawkes process with $\mu = 0.01$, on the right, a raster plot of the same process.

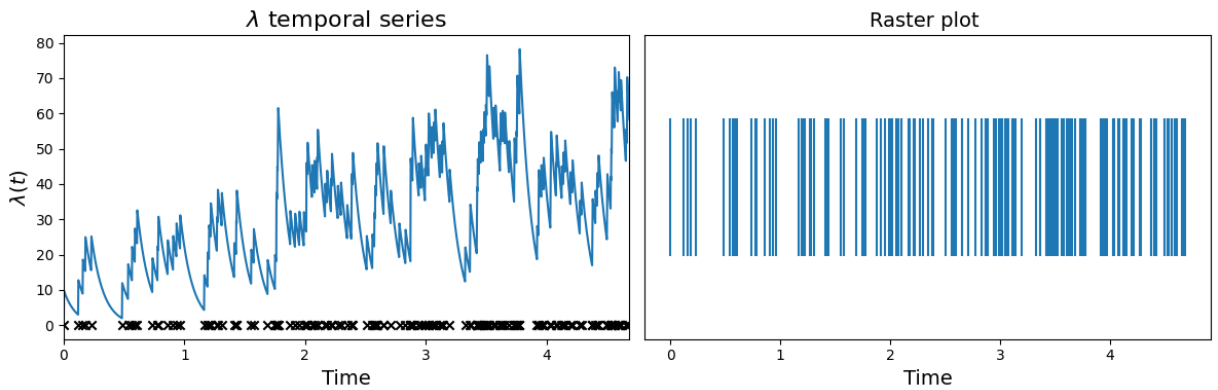


Figure 1.7. On the left, a temporal series of $K = 150$ events of a Hawkes process with $\mu = 0.01$, on the right, a raster plot of the same process.

As shown in Figure 1.6, when the background rate is smaller than 1, events are less likely to occur, but when they do, they tend to form avalanches of activity thanks to the self-excitation. On the other

hand, when the background rate is greater than 1, events occur more frequently, forming avalanches of activity more frequently and longer, as shown in Figure 1.7. If we ignore the time of occurrence of the events and we focus only on the structure of λ and therefore of the events, we can see that the process with $\mu = 0.01$ has a bursty structure, while the process with $\mu = 10$ has a more regular structure. This phenomenon is exposed in Figures 1.8 and 1.9.

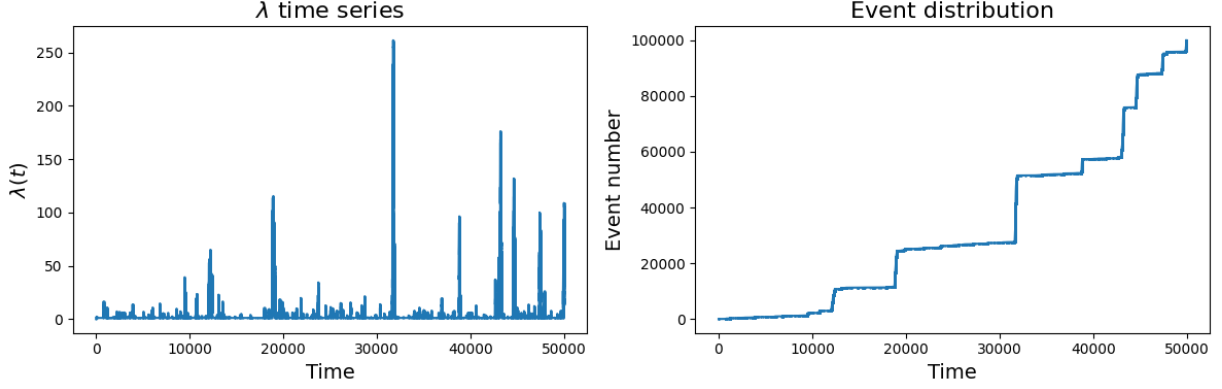


Figure 1.8. First, a temporal series of $K = 10^5$ events of a Hawkes process with $\mu = 0.01$, on the left, the event distribution.

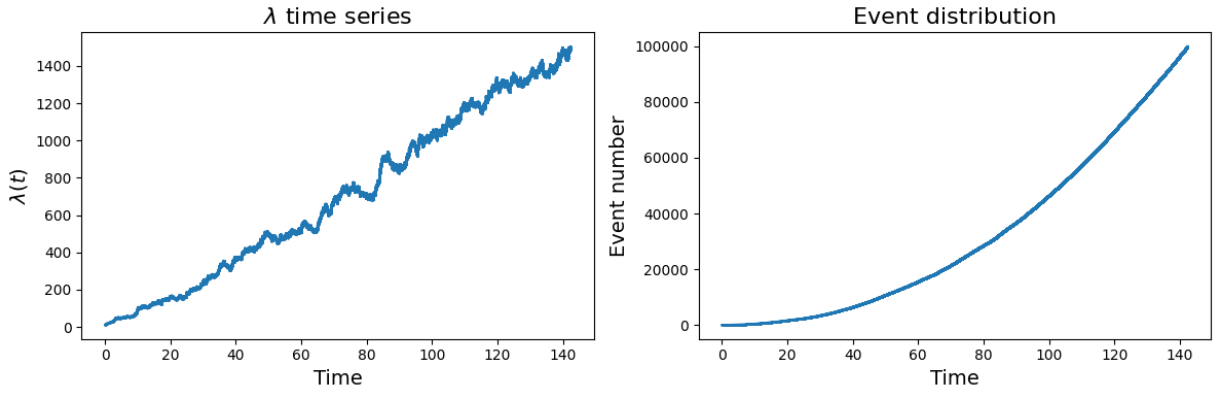


Figure 1.9. First, a temporal series of $K = 10^5$ events of a Hawkes process with $\mu = 10$, on the left, the event distribution.

In most cases, the motivation of study of point processes is counting the events, but in our case we also are interested in the time of occurrence of the events which will let us define bursts or avalanches of activity that we will use to describe the dynamics of the system. As we have said previously $\alpha = 1$, $\beta = 1$, making n the parameter that controls the weight of the self-excitation. Essentially, n and α play the same role, so we will use them indistinctly. The previous figures showed the dynamics for $n = 1$, making the system critical as a critical branching process PONER ALGO AQUÍ EN REFERENCIA A LA SECCIÓN ANTERIOR [9]. , but we will also study the dynamics for $n = 2$ and two coupled Hawkes processes.

Hawkes processes with $n = 2$

In this case, the self-excitation does not lead to a critical dynamic, but to a supercritical dynamic. In this situation, the time until the first event occur is given in mean by μ^{-1} , after it occurs, an avalanche of activity starts as shown in Figure 1.10.

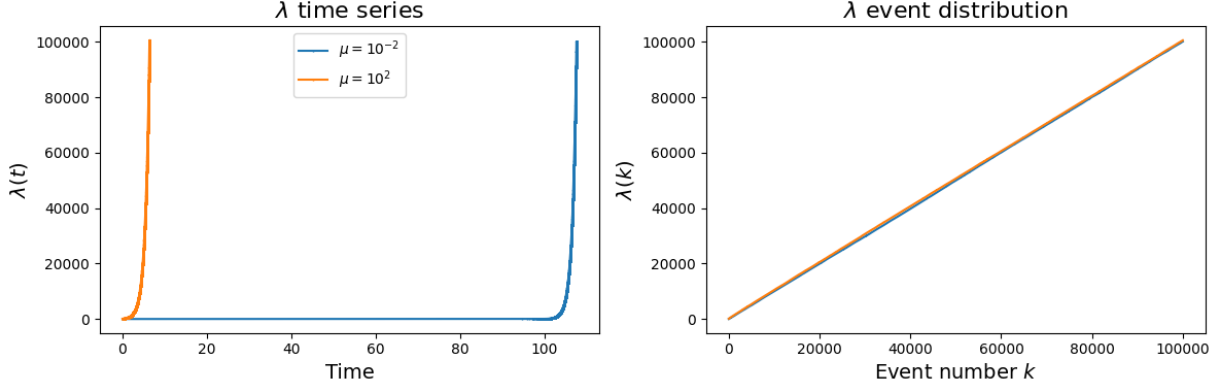


Figure 1.10. On the left, a temporal series of $K = 10^5$ events of a Hawkes process with $\mu \in \{10^{-2}, 10^2\}$ and $n = 2$, on the right, the λ distribution versus the event number.

As expected, after the first event, we have an exponential increase in time and a linear increase in the number of events for the rate. This behaviour will change also the structure of the raster plots, which are where we will get the dynamics information. In Figures 1.11(a) and 1.11(b) two raster plots are shown for the two different background intensities.

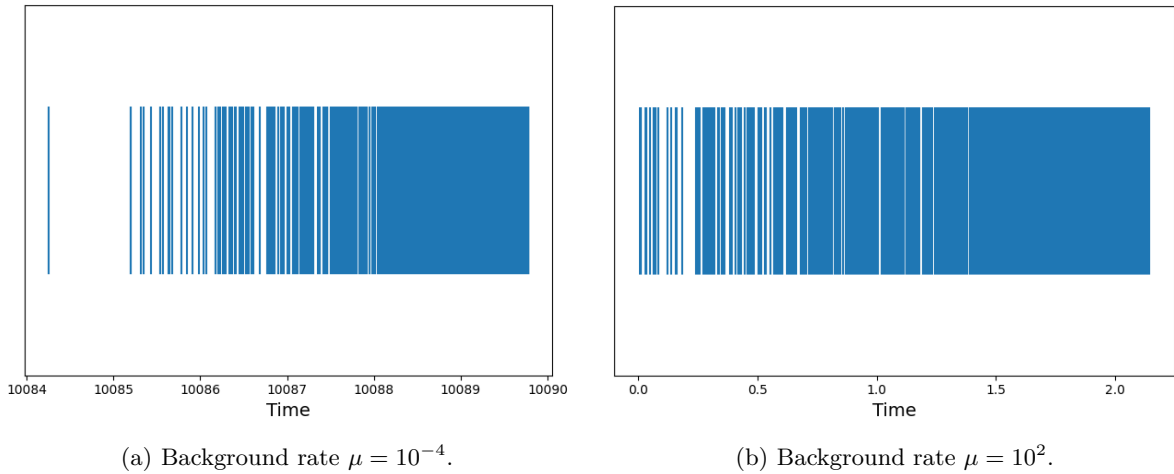


Figure 1.11. Raster plots of Hawkes processes with $n = 2$. In both cases, the number of events is $K = 10^3$, they also have the same structure, the first event, on average, happens in $\mu^{-1} a.u.$ of time; then, an avalanche of events takes place.

Coupled Hawkes processes

With the previous knowledge, we can model an isolated neuron working in different regimes, but as we know, the brain is composed of an enormous amount of neurons connected to each other forming a network. Moreover, neurons can be classified into two kinds, excitatory and inhibitory neurons. To get closer to modelling the brain, we will also generate two coupled Hawkes processes, one corresponding to an excitatory population and the other to an inhibitory population or just an excitatory and inhibitory neuron. Both populations (neuron) will have a background rate μ_E and μ_I , and they will be able to interact with each other and with themselves, the “strength” of the interactions will be controlled by the parameters n_{EE} , n_{EI} , n_{IE} and n_{II} . In most cases, the auto-inhibition can be considered negligible. These interactions are illustrated in Figure 1.12.

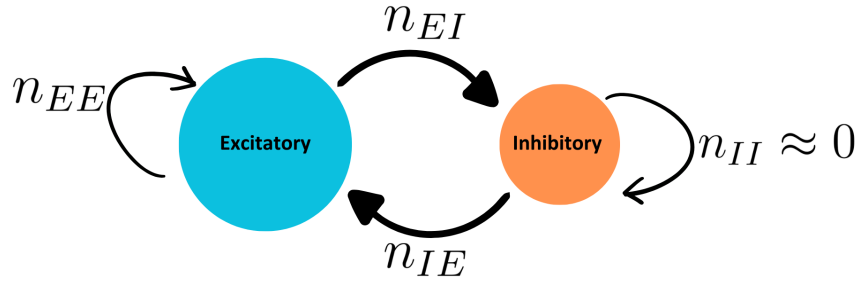


Figure 1.12. Scheme of the interaction between the excitatory and inhibitory populations. As illustrated, the excitatory population can excite itself and the inhibitory population, while the inhibitory population can only inhibit the excitatory population, because on most cases the auto-inhibition is negligible [17].

In a similar way to the previous cases, the background rates will only change time until the first event occurs, but signals will only rely on the “strength” $n_{i,j}$ of the interactions. Studying this parameter space, the different phases and the respective avalanche statistics could be a Master’s thesis in itself. That is why we will only look at a couple parameter configurations. The first one gives us a pseudo-critical signal, regulated by the inhibition. On the other hand, the second one gives us an oscillatory stable signal. For both signals, the background rates will be $\mu_E = \mu_I = 0.01$, the other interaction parameters are shown in Table 1.1.

Table 1.1. Interaction parameters for both bivariate processes

	Pseudo-critical	Stable
n_{EE}	1.5	1.5
n_{EI}	1.5	1.5
n_{IE}	-0.33	-0.5
n_{II}	0	0

With the values of n_{EE} and n_{EI} , the signals would be supercritical, but adding the inhibition, the

comportment will be totally different. Moreover, we will see that a slight change in the inhibition strength will change the signal from pseudo-critical to oscillatory. In Figures 1.13 and 1.14 are presented time series and raster plots for the two different signals.

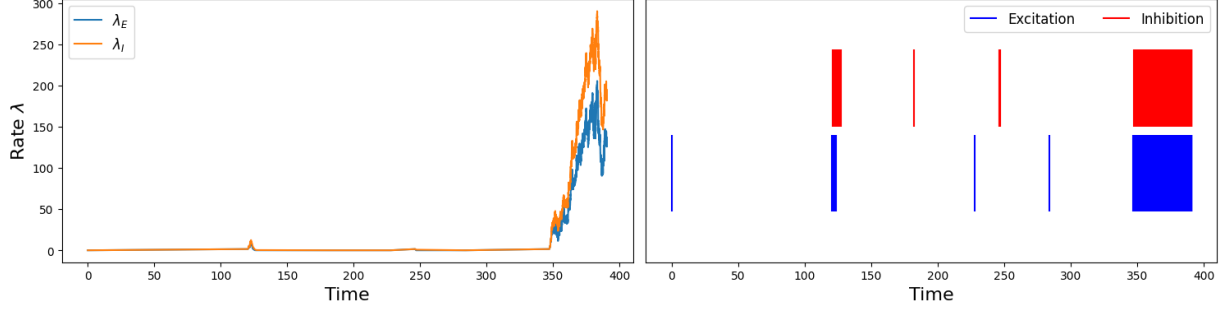


Figure 1.13. On the left, a temporal series of $K = 10^4$ events of a bivariate Hawkes process with the interaction parameters of the pseudo-critical signal shown in Table 1.1, on the right, the raster plot of the same process for excitatory and inhibitory events.

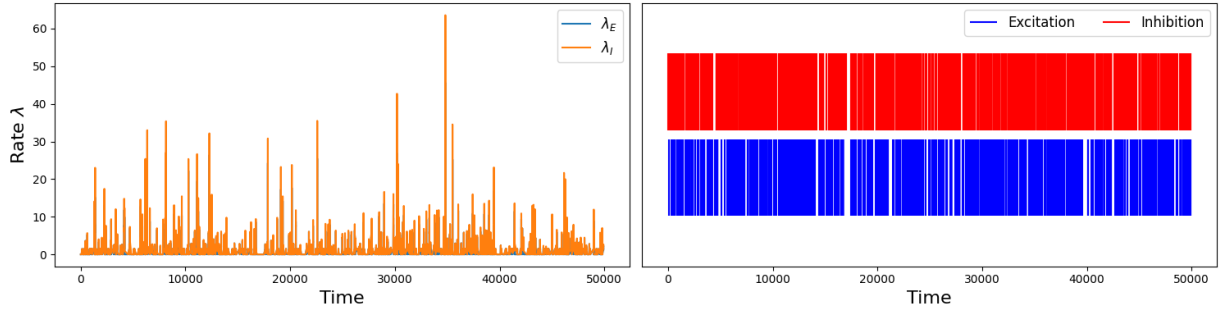


Figure 1.14. On the left, a temporal series of $K = 10^4$ events of a bivariate Hawkes process with the interaction parameters of the “stable” signal shown in Table 1.1, on the right, the raster plot of the same process for excitatory and inhibitory events.

As illustrated, the pseudo-critical signal has a bursty structure until a big avalanche of activity occurs, on the contrary, the oscillatory signal has a more regular structure. Later on, in Chapter 4 we will see how this difference in the structure of the signals affects the avalanche statistics.

Chapter 2

Objectives

The main objectives of this Master's thesis are:

- To understand the basics of criticality and its appearance in living systems, particularly in the brain.
- To understand what Hawkes processes are, where we can find them, how to generate them computationally and relate them with neuroscience.
- To understand the importance of time binning and reproduce the results of the original paper. [9] and compare them with the results obtained in this work.
- To study the behaviour of a supercritical self-exciting process and compare it with the results from a critical process.
- To study how an excitatory and inhibitory coupled Hawkes process behave.

Chapter 3

Methodology

In the following sections, the methodology for data generation, management and analysis will be presented. To address these issues, we will use Python [18, 19] due to its versatility and the wide range of libraries available. The two used will be NumPy [20] and Matplotlib [21] for the visualization.

3.1 Time series factory

The first step is the generation of time series, there are two ways to do this: the slow one and the fast one. The first one is discretizing the time and calculating the rate at each time step according with Eq. 1.2, then accept or reject the event if $p < \lambda \cdot dt$ for a random number $p \in \mathcal{U}[0, 1]$. This method works for small time series, but for large ones is not efficient because the summation of the kernel function has to be done at each time step. The pseudo-code for this method is presented in Algorithm 1.

Algorithm 1 Slow method to generate Hawkes processes.

Require: t_{max} , $n_{intervals}$, $\lambda(t_0) = \mu$, p

```
dt ←  $\frac{t_{max}}{n_{intervals}}$ 
for  $i = 0$  to  $n_{intervals}$  do1
     $\lambda(t_k) \leftarrow \mu + n \sum_{t_i < t_k} \phi(t_k - t_i)$   $\triangleright t_i = i \cdot dt$ 
    if  $\lambda(t_k) \cdot dt > p$  then
         $t_{event} \leftarrow t_k$ 
    end if
end for
```

The fast method takes advantage of Monte Carlo methods [22] to generate the time series. The idea of this procedure consists in computing the inter-event time instead of the time of the event. To get to the algorithm, we start from the following expression:

$$PDF(\text{inter-event time} = \Delta t) = \lambda(t + \Delta t) e^{-\int_t^{t+\Delta t} \lambda(t') dt'} \quad (3.1)$$

To demonstrate this, we have to take a look at the Figure 3.1 and recall that λ is a probability per unit of time.

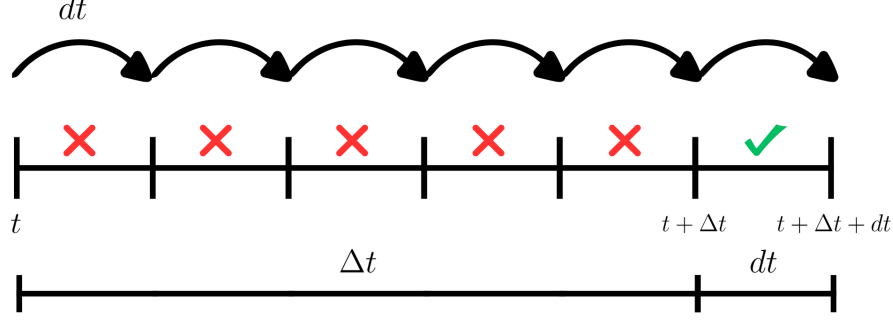


Figure 3.1. Diagram to calculate the cumulative probability of the inter-event time.

The probability per unit of time of having an event in the interval $[t + \Delta t, t + \Delta t + dt]$ is the probability of no events in the interval $[t, t + \Delta t]$ times the probability of happening in the interval $[t + \Delta t, t + \Delta t + dt]$. Putting words into mathematics, we have that the probability of not having an event in the interval $[t, t + \Delta t]$ is:

$$\begin{aligned}
 P(\text{event} \in [t + \Delta t + dt]) &= (1 - \lambda(0) \cdot dt) (1 - \lambda(dt) \cdot dt) (1 - \lambda(2dt) \cdot dt) \dots \\
 &= \prod_{k=0}^{\infty} \underbrace{(1 - \lambda(kdt) \cdot dt)}_{e^{\ln(1 - \lambda(kdt)dt)}} = e^{\sum_{k=0}^{\infty} \ln(1 - \lambda(kdt)dt)} = \dots \quad \text{Using } \ln(1 - \varepsilon) \approx -\varepsilon \\
 &= e^{-\sum_{k=0}^{\infty} \lambda(kdt)dt} \underset{dt \rightarrow 0}{=} e^{-\int_t^{t+\Delta t} \lambda(t')dt'}.
 \end{aligned} \tag{3.2}$$

Knowing that the probability of having an event in the interval $[t + \Delta t, t + \Delta t + dt]$ is $\lambda(t + \Delta t)dt$, we have:

$$P(\text{event} \in [t + \Delta t, t + \Delta t + dt])dt = \lambda(t + \Delta t)dt \cdot e^{-\int_t^{t+\Delta t} \lambda(t')dt'} \times PDF(\text{inter-event time} = \Delta t)dt. \tag{3.3}$$

Having that we can calculate the inter-event time following the next steps.

$$PDF(\text{inter-event time} = \Delta, t) = \lambda(t + \Delta t) \times \underbrace{e^{\int_t^{t+\Delta t} \lambda(t')dt'}}_{\text{No events during } (t, t+\Delta t)}$$

In order to generate Δt , we will use the inverse transform method [23], therefore we have to calculate the cumulative probability of the inter-event time:

$$\begin{aligned}
 \text{accum}(\Delta t) &= \int_0^{\Delta t} PDF(\Delta t') d\Delta t' = u \in \mathcal{U}[0, 1] \\
 &= \int_0^{\Delta t} \underbrace{\lambda(t + \Delta t') e^{\int_t^{t+\Delta t'} \lambda(t')dt'}}_{-\frac{d}{d\Delta t'} \left[e^{-\int_t^{t+\Delta t} \lambda(t')dt'} \right]} d\Delta t' = u \quad \text{Using Barrow rule} \\
 &= e^{-\int_t^{t+\Delta t} \lambda(t')dt'} \Big|_0^{\Delta t} = 1 - e^{-\int_t^{t+\Delta t} \lambda(t')dt'} = u \quad \text{Taking logarithms} \\
 &\int_t^{t+\Delta t} \lambda(t')dt' = -\ln(1 - u) = \ln(\bar{u})
 \end{aligned} \tag{3.4}$$

To compute the inter-event time, we have to generate $\bar{u} \sim$ and solve the equation. Having in mind this relation and using Eq. 1.4 we have:

$$\begin{aligned}
u &= 1 - e^{-\mu(t-t_k)} e^{-\left(\lambda(t_k) + \alpha - \mu\right) \cdot \overbrace{\int_{t_k}^t e^{-\beta(t'-t_k)} dt'}^{-\frac{1}{\beta} [e^{-\beta(t-t_k)} - 1]}} \\
u &= 1 - \underbrace{e^{-\mu(t-t_k)}}_{P(t_{k+1}^{(1)} > t)} \underbrace{e^{-\left[(\lambda(t_k) + \alpha - \mu)\beta^{-1} (1 - e^{-\beta(t-t_k)})\right]}}_{P(t_{k+1}^{(2)} > t)}
\end{aligned} \tag{3.5}$$

Then we apply the composition method [15]. If we take $t_{k+1} = \min(t_{k+1}^{(1)}, t_{k+1}^{(2)})$; then $t_{k+1} \sim P(t_{k+1} > t)$, hence:

$$\begin{aligned}
\text{Prob}(t_{k+1} = \min(t_{k+1}^{(1)}, t_{k+1}^{(2)}) \leq t) &= 1 - \text{Prob}\left(\min(t_{k+1}^{(1)}, t_{k+1}^{(2)}) > t\right) \\
&= 1 - \text{Prob}(t_{k+1}^{(1)} > t) \cdot \text{Prob}(t_{k+1}^{(2)} > t)
\end{aligned} \tag{3.6}$$

where we have used that the probability that the smaller is greater than t is that each separately is greater than t because both have to be greater than t . As we can see the expressions in Eqs. 3.5 and 3.6 are the same, so we can use the composition method to generate the inter-event time. Then, the algorithm to generate the inter-event time is:

1. Generate $t_{k+1}^{(1)} \sim P(t_{k+1}^{(1)} > t) = e^{-\mu(t-t_k)}$ using

$$P(t_{k+1}^{(1)} \leq t) = 1 - \underbrace{e^{-\mu(t-t_k)}}_{\substack{\bar{u}_1 \in \mathcal{U}[0,1] \\ 1-\bar{u}_1 = u_1}} = u_1 \in \mathcal{U}[0, 1]$$

This is done by generating $u_1 \in \mathcal{U}[0, 1]$ and solving the equation.

$$\begin{aligned}
u_1 &= 1 - e^{-\mu(t_{k+1}^{(1)} - t_k)} \\
\ln(u_1) &= -\mu(t_{k+1}^{(1)} - t_k) \Rightarrow t_{k+1}^{(1)} = t_k - \frac{\ln(u_1)}{\mu}
\end{aligned} \tag{3.7}$$

2. Generate $t_{k+1}^{(2)} \sim P(t_{k+1}^{(2)} > t) = e^{-\left((\lambda(t_k) + \alpha - \mu)\beta^{-1} \left(1 - e^{-\beta(t_{k+1}^{(2)} - t_k)}\right)\right)}$ in a similar way as before:

$$\begin{aligned}
u_2 &= 1 - e^{-\left((\lambda(t_k) + \alpha - \mu)\beta^{-1} \left(1 - e^{-\beta(t_{k+1}^{(2)} - t_k)}\right)\right)} \\
-\ln(u_2) &= \left((\lambda(t_k) + \alpha - \mu)\beta^{-1} \left(1 - e^{-\beta(t_{k+1}^{(2)} - t_k)}\right)\right) \\
1 + \frac{\beta \ln u_2}{\lambda(t_k) + \alpha - \mu} &= e^{-\beta(t_{k+1}^{(2)} - t_k)} \\
t_{k+1}^{(2)} &= t_k - \beta^{-1} \ln \underbrace{\left(1 + \frac{\beta \ln u_2}{\lambda(t_k) + \alpha - \mu}\right)}_{\text{This number must be positive}}
\end{aligned} \tag{3.8}$$

3. Choose $t_{k+1} = \min \left(t_{k+1}^{(1)}, t_{k+1}^{(2)} \right)$
4. Calculate the rate at t_{k+1} using Eq. 1.3 and go back to step 1.

With this method, we can generate time series efficiently. The pseudo-code for this method is presented in Algorithm 2.

Algorithm 2 Algorithm to generate K Hawkes events.

Require: $\alpha, \beta, \lambda(t_0) = \mu, K$
for $k = 0$ to K **do**
 $u_1, u_2 \leftarrow \mathcal{U}[0, 1]$
 $t_{k+1}^{(1)} \leftarrow \frac{\ln(u_1)}{\mu}$
 $t_{k+1}^{(2)} \leftarrow \beta^{-1} \ln \left(1 + \frac{\beta \ln u_2}{\lambda(t_k) + \alpha - \mu} \right)$
 $t_{k+1} \leftarrow \min \left(t_{k+1}^{(1)}, t_{k+1}^{(2)} \right)$
 $\lambda(t_{k+1}) \leftarrow \mu + e^{-\beta(t_{k+1}-t_k)} (\lambda(t_k) - \mu + n)$
end for

To conclude generation of time series section, we can generalise the algorithm in order to generate M Hawkes processes coupled [15, 16]. The essence of the algorithm is the same as the one presented. First, we generate the inter-event time for the excitatory population and the inhibitory population, after that, we choose the minimum of both and update the rates of both populations according to the event that has just occurred. Mathematically it is expressed as follows:

1. Generate $\Delta_{k+1} = \min \left\{ \Delta_{k+1}^{(1)}, \Delta_{k+1}^{(2)} \right\}$ with $\Delta_{k+1}^{(j)} = t_{k+1}^{(j)} - t_k^{(j)}$ generated as in Eqs. 3.7 and 3.8.

$$\Delta_{k+1}^{(j)} = \min \left\{ -\frac{\ln(u_1^{(j)})}{\mu_j}, -\beta_j^{-1} \ln \left(1 + \frac{\beta_j \ln u_2^{(j)}}{\underbrace{\lambda_j(t_k^{(j)}) + \alpha_j - \mu_j}_{g_j}} \right) \right\} \quad (3.9)$$

Note that g_j must be positive, otherwise, take the other term.

2. Once we have the process (l), we update the time for the following event as $t_{k+1} = t_k + \Delta_{k+1}^{(l)}$.
3. Update the rates for the excitatory and inhibitory populations as follows:

$$\lambda_j(t_{k+1}) = \mu_j + e^{-\beta_j(t_{k+1}-t_k)} (\lambda_j(t_k) - \mu_j + \alpha_{l \rightarrow j}) \quad \text{with } j = 1, 2 \quad (3.10)$$

The pseudo-code for this method is presented in Algorithm 3.

Algorithm 3 Algorithm to generate K Hawkes events for two coupled processes.

Require: $\alpha_{11}, \alpha_{12}, \beta_1, \mu_1, \alpha_{22}, \alpha_{21}, \beta_2, \mu_2, K$

for $k = 0$ to K **do**

$u_1^{(1)}, u_2^{(1)}, u_1^{(2)}, u_2^{(2)} \leftarrow \mathcal{U}[0, 1]$

$\Delta_{k+1}^{(1)} \leftarrow \min \left(-\frac{\ln(u_1^{(1)})}{\mu_1}, -\beta_1^{-1} \ln \left(1 + \frac{\beta_1 \ln u_2^{(1)}}{\lambda_1(t_k) + \alpha_{11} - \mu_1} \right) \right)$

$\Delta_{k+1}^{(2)} \leftarrow \min \left(-\frac{\ln(u_1^{(2)})}{\mu_2}, -\beta_2^{-1} \ln \left(1 + \frac{\beta_2 \ln u_2^{(2)}}{\lambda_2(t_k) + \alpha_{22} - \mu_2} \right) \right)$

$l \leftarrow \arg \min (\Delta_{k+1}^{(1)}, \Delta_{k+1}^{(2)})$

$t_{k+1} \leftarrow t_k + \Delta_{k+1}^{(l)}$

$\lambda_1(t_{k+1}) \leftarrow \mu_1 + e^{-\beta_1(t_{k+1}-t_k)} (\lambda_1(t_k) - \mu_1 + \alpha_{l \rightarrow 1})$

$\lambda_2(t_{k+1}) \leftarrow \mu_2 + e^{-\beta_2(t_{k+1}-t_k)} (\lambda_2(t_k) - \mu_2 + \alpha_{l \rightarrow 2})$

end for

3.2 When physics and cooking merge

Now we have a method to generate the main ingredient, time series. In order to cook (analyze) them, our tools will be Python libraries and a control parameter, which in our case will be a resolution parameter $\Delta > 0$ that will allow us to identify clusters of activity. Assuming that we have a time series with K events that happen in times $\{t_1, \dots, t_K\}$. Each event starts a cluster and the following event will be part of this cluster if the time between both events is less than Δ and so on for the rest. We define the size of the cluster as the number of events in the interval $[t_{first}, t_{last}]$ and its duration as $t_{last} - t_{first}$. The extreme cases are when Δ is smaller than the minimum inter-event time, where each event is a cluster of size 1 and duration 0. The other extreme is when Δ is greater than the largest inter-event time, where all the events are in the same cluster of size K and duration $t_K - t_1$. Between these two extremes, we will have different regimes of the process. Our recipe will be the phase diagram, specifically the percolation diagram, where we will plot the percolation strength P_∞ as a function of the resolution parameter Δ . The percolation strength is defined as the fraction of events that are in the largest cluster over the total number of events. Three different set of parameters will be used to generate the time series in order to compare them. The parameters α and β will be fixed to unless otherwise stated, the other parameters are shown in Table 3.1. Once we got our recipe (the percolation diagram), we should be able to identify the critical points and the different regimes of the process. By carefully choosing Δ from the percolation diagram, we will be able to identify the different regimes with their respective power law exponentes.

Table 3.1. Configuration of the parameters for the simulations of the article [9].

Configuration	μ	n
First	1	0
Second	10^{-4}	1
Third	10^2	1

The percolation diagram will be generated by generating 1000 time series for each configuration and calculating the percolation strength for each one because in general they are not stationary processes as we can observe in Figure 3.2.

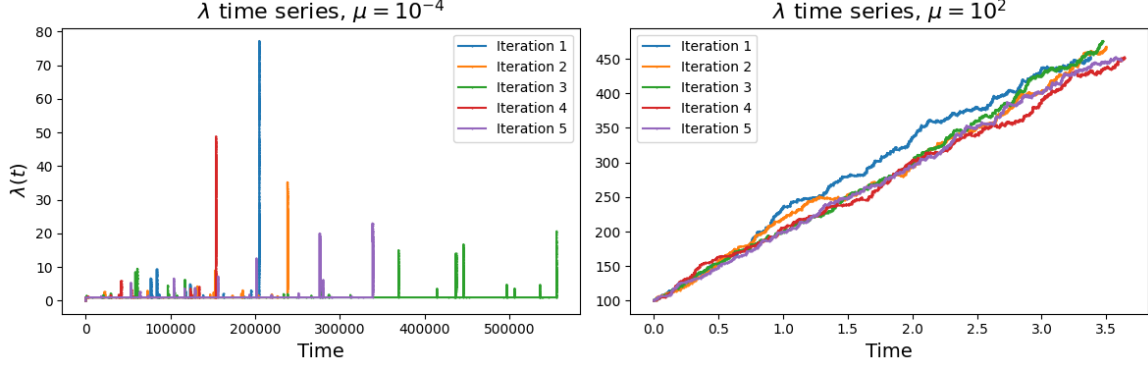


Figure 3.2. Five a temporal series of $K = 10^5$ events of Hawkes processes with $\mu = 10^{-4}$ on the left side and $\mu = 10^2$ on the right one.

Beginning with the first configuration, we have an homogeneous Poisson process which we know that its interevent time will be distributed randomly with a probability of having an inter-event time x_i given by $P(x_i) = \mu e^{-\mu x_i}$. Consequently, two consecutive events will be a part of a cluster fixing the resolution parameter to Δ with a probability of

$$P(x_i \leq \Delta) = 1 - e^{-\mu \Delta} \quad \forall i. \quad (3.11)$$

This represents the probability in a homogeneous 1D percolation model [10], where we can identify a non percolant phase and a percolant phase separated by the critical point Δ^* . We can calculate this parameter if we know the maximum inter-event time of the time series. Let us assume that our time series has K events, therefore, it will percolate if the condition we have just established is satisfied. We can calculate this threshold as the average of the maximum inter-event time in K samples from the inter-event time distribution solving the following equation:

$$\begin{aligned} K \int_{\Delta^*}^{\infty} P(x) dx &= 1 \\ K \int_{\Delta^*}^{\infty} \mu e^{-\mu x} dx &= 1 \\ -K [e^{-\mu x}]_{\Delta^*}^{\infty} &= K \left[e^{-\mu \Delta^*} - \cancel{e^{-\mu \infty}} \right] = 1 \\ K e^{-\mu \Delta^*} &= 1 \\ \Delta^*(K) &= -\frac{\ln(K)}{\mu} \end{aligned} \quad (3.12)$$

For the other two configurations, on both we have a self-exciting process with $n = 0$, which means that we have a critical dynamical regime as we shall see later but with different background rates, one much smaller than 1 and the other much greater than 1. This fact will be reflected in the percolation diagram. We will not approach this cases from a theoretical point of view but from a graphic one. With the second configuration, as we have seen in Figure 1.8 if the condition $\mu \ll 1$ is satisfied, we will

have a bursty structure in the time series. Due to the low background rate, the events are less likely to occur, but when they do, they tend to form avalanches of activity thanks to the self-excitation. This will be reflected in the percolation diagram as a first phase transition at a critical point Δ_1^* when Δ is of the order of the average cluster size. Then, a second phase transition will occur at a critical point Δ_2^* when Δ is greater than the greatest inter-event time. This phenomena is illustrated in Figure 3.3.

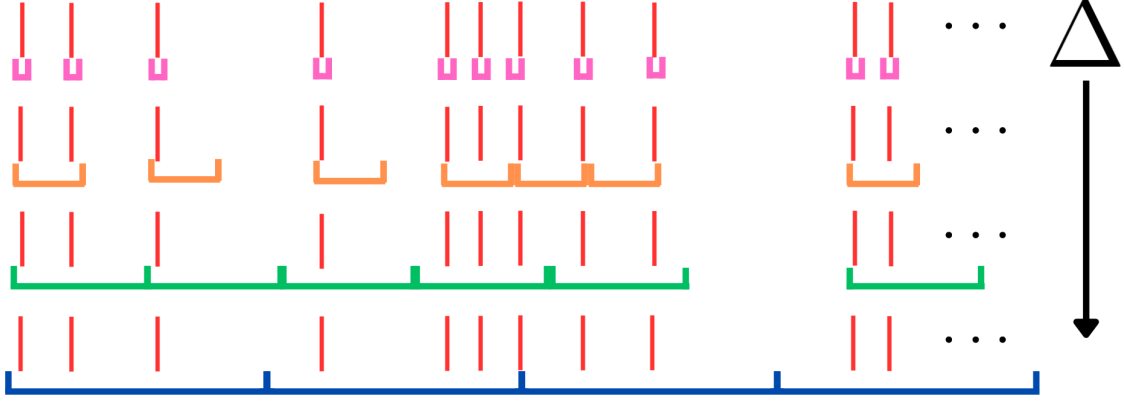


Figure 3.3. Diagram for $\mu \ll 1$. Red lines represent the events, clusters are coloured. As we can see, we have two regimes, one when Δ is of the order of the average cluster size and another when is of the order of the inter-event time where the system percolates.

On the other hand, when $\mu \gg 1$ events occur more frequently, without making the bursty structure of Figure 1.8, but making a more regular structure as illustrated in Figure 1.9. This will be reflected in the phase diagram as a single phase transition at a critical point Δ^* when Δ is of the order of the average cluster size. This phenomena is illustrated in Figure 3.4. Note the absence of a time scale in both diagram, they are diagrams for the explanation of the phase diagram.

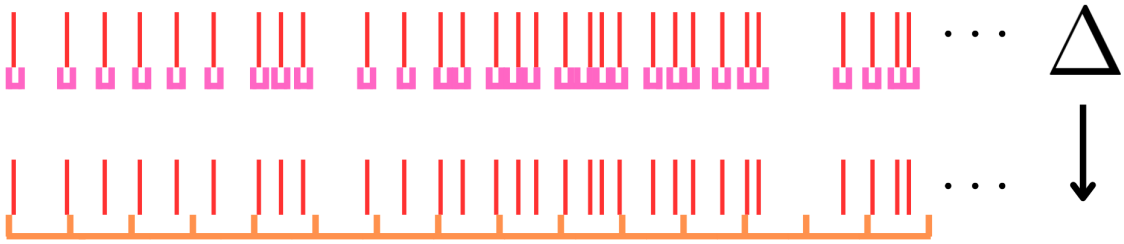


Figure 3.4. Diagram for $\mu \gg 1$. Red lines represent the events, clusters are coloured. In this situation, events occur more regularly, resulting in a unique transition corresponding the case of Δ is similar to the inter-event time producing the system percolation.

Chapter 4

Results

This section provides the main results of the investigation. The main functions used to obtain these results are shown in the Appendix A. The results are divided into three sections:

1. First, the results reproduced from the original paper [9] are presented.
2. Secondly, we will present the same analysis for the case of a Hawkes process with $n = 2$.
3. Finally, we will study the behaviour of two Hawkes processes couples, one representing an excitatory neuron and the other an inhibitory neuron.

4.1 Results from the original paper

The structure for the three sections will be the same. First, we will obtain the phase diagram for the percolation strength P_∞ versus our control parameter, the resolution parameter Δ , obtaining the critical(s) point(s) Δ_i^* . Having these in knowledge, the avalanche statistics for the size and duration will be studied for different regions of the phase diagram.

As previously stated, the first result is the percolation phase diagram, shown in Figure 4.1. It displays the percolation strength P_∞ , which is the number of events in the largest cluster divided by the total number of events of the time series versus the resolution parameter Δ . We will generate several time series, compute the percolation strength for each one and take the average value.

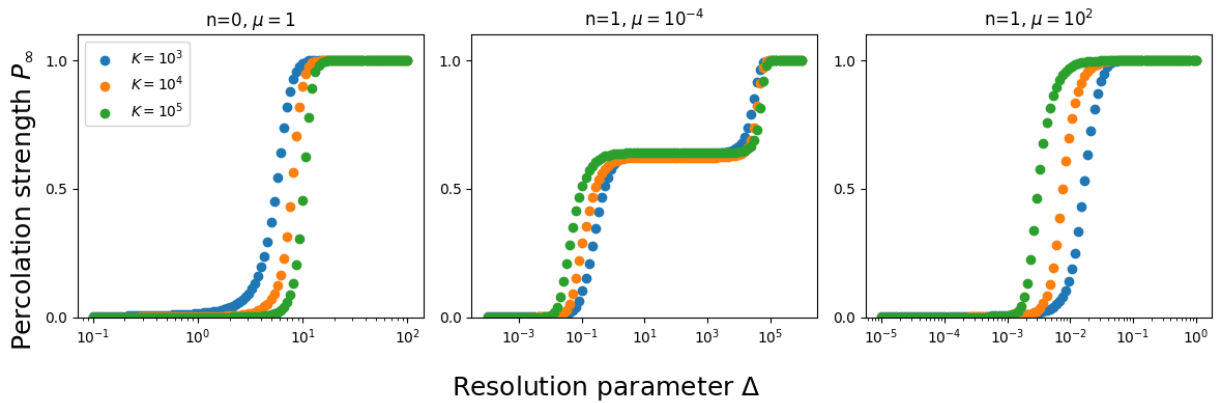


Figure 4.1. Percolation phase diagrams for different event number K taking average values of $R = 1000$ realizations.

The first plot configuration is a homogeneous Poisson process with rate $\mu = 1$ which we have overviewed in Section 1.2.1 and has a pseudocritical threshold at $\Delta^*(K) = \frac{\ln(K)}{\mu}$ as we have demonstrated in Section 3.2. Due to the fact of finite size of the time series, the transition is discontinuous at the threshold, as expected for 1D percolation [10].

Now, we contemplate Hawkes processes, for the first case ($\mu = 10^{-4}$), we can observe a double discontinuous transition. The first one at Δ_1^* and the second one at Δ_2^* . As we are going to see with the avalanche statistics, the first transition is associated with the universality class of 1D percolation whose exponents are $\alpha = \tau = 2$. On the other hand, the second transition is associated with the universality class of mean-field branching process whose exponents are $\alpha = 3/2$ and $\tau = 2$. This double transition is also compatible with the fact mentioned in Figure 3.3. We can also observe that the plateau between the two transitions is wider as the K increases as expected. For the second case ($\mu = 10^2$), similarly to the first one, we have a single discontinuous transition at Δ_1^* associated with the universality class of 1D percolation as well, this phenomenon is also compatible with the one shown in Figure 3.4.

Another interesting analysis to characterize the phases is studying the susceptibility χ . In this case, it is defined by Eq. 4.1.

$$\begin{aligned}\chi &= \frac{\langle S_M^2 \rangle - \langle S_M \rangle^2}{\langle S_M \rangle} \\ &= K \cdot \frac{\langle P_\infty^2 \rangle - \langle P_\infty \rangle^2}{\langle P_\infty \rangle} \\ &= K \cdot \frac{\sigma^2(P_\infty)}{\langle P_\infty \rangle}\end{aligned}\tag{4.1}$$

The susceptibility (normalized to the number of events) is shown in Figure 4.2. For the Poisson process, we see that the susceptibility has a peak at the threshold $\Delta^*(K)$, then it vanishes as expected. For the Hawkes case with $\mu = 10^{-4}$, we observe that χ has a peak at the critical point Δ_1^* , then we have a critical behaviour where the susceptibility is not zero at the plateau $[\Delta_1^*, \Delta_2^*]$ and finally, it vanishes at the second critical point Δ_2^* . Finally, for the Hawkes case with $\mu = 10^2$ and likewise the Poisson process, the susceptibility has a divergence at the critical point Δ_1^* and then it vanishes.

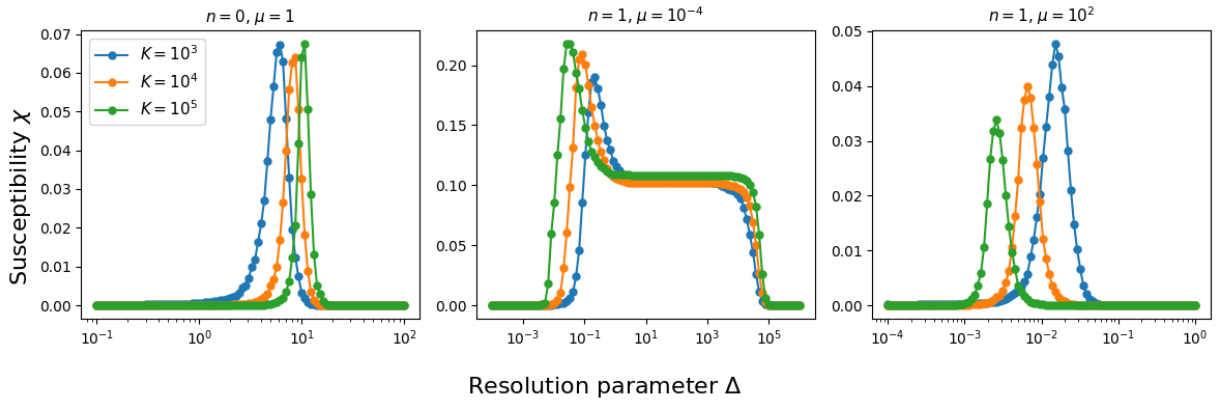


Figure 4.2. Susceptibility χ normalized to the number of events K , for different event number K and taking average values for $R = 1000$ realizations.

Once we have the phase diagram, we can study avalanche statistics, but first, we need to obtain the thresholds Δ_1^* and Δ_2^* from the phase diagram. The article [9] provides the following formulas to compute these thresholds for the Hawkes process with $\mu = 10^{-4}$ and:

$$\Delta_1^* \simeq \frac{\ln(K)}{\langle \lambda \rangle} = \frac{\ln(K)}{\mu + \sqrt{2\mu K}} \quad (4.2)$$

$$\Delta_2^* = \frac{\ln(K)}{\mu} \quad (4.3)$$

and for $\mu = 10^2$:

$$\Delta_1^* = \frac{\ln(K)}{\mu} \quad (4.4)$$

Bearing this in mind and the definitions of the size and duration of avalanches established in the previous chapter, we can study the avalanches for the different regions of the phase diagram. We just are going to show the results for $\mu = 10^{-4}$ and for $\mu = 10^2$ in Figure 4.3. The Poisson process behaviour can be found in [10, 24].

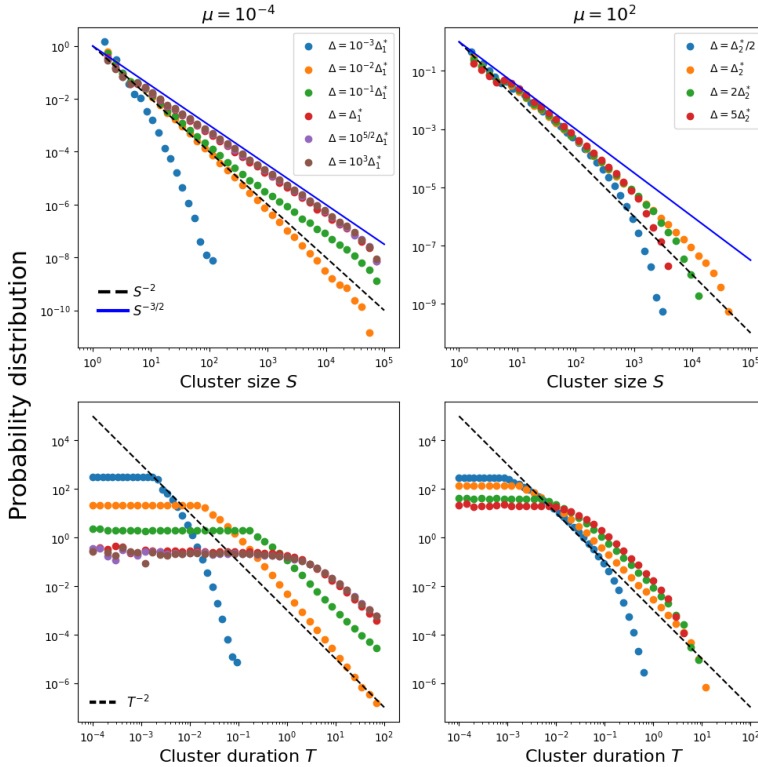


Figure 4.3. Avalanche analysis for Hawkes process with $n = 1$, $K = 10^5$ events. The histograms have been calculated over $R = 1000$ time series.

As a consequence of the huge simulation time of time series of $K = 10^8$ events, we have only studied the avalanches for $K = 10^5$, moreover, we have taken other criterion to obtain the histograms. Instead of considering $C = 10^7$ clusters, we have obtained the histograms of $R = 1000$ time series. This leads to a different amount of clusters for each value of Δ , nevertheless, we have obtained equivalent and reliable results.

For $\mu = 10^{-4}$, the probability distribution of the cluster size and duration shows three different behaviours. For $\Delta \ll \Delta_1^*$, the behaviour is subcritical, leading to an exponential decay for the size and duration. While we increase Δ , we reach the critical point where the exponents are $\alpha = \tau = 2$ compatible with the universality class of 1D percolation. After that, we reach the plateau $[\Delta_1^*, \Delta_2^*]$ where we have a crossover to the universality class of mean-field branching process and 1D percolation.

Finally, for $\Delta \rightarrow \Delta_2^*$, we obtain the universality class of mean-field branching process

exponents $\alpha = 3/2$ and $\tau = 2$. For $\mu = 10^2$, the plots show a power-law distribution for both cluster size and duration with exponents $\alpha = \tau = 2$ corresponding to the universality class of 1D percolation as we have mentioned before.

Note that we have reproduced the same behaviour, but for other values of Δ , specifically, for two order of magnitude less than article value. This is due to the fact that Eq. 4.2 needs the assumption of large time series, condition which is not fulfilled in our case. We can illustrate this difference for example in the susceptibility diagram, where the peak should be at Δ_1^* , but in our case, it is at $\Delta_1^*/100$ as shown in Figure 4.4.

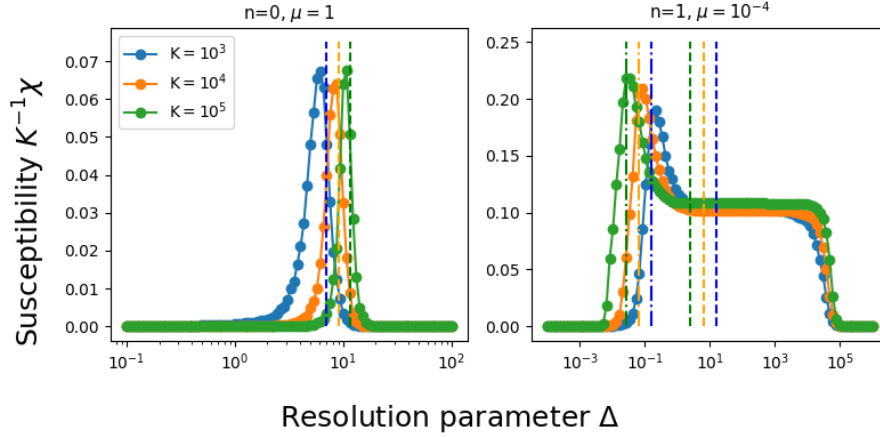


Figure 4.4. At the left, the vertical dashed lines represent the critical points $\Delta^*(K)$ for the Poisson process. At the right, the vertical dashed lines represent the critical points $\Delta_1^*(K)$ given by Eq. 4.2 and the dotted dashed lines the $\Delta_1^*/100$.

4.2 Results for n=2

In the article, the authors have studied a process which is critical itself because the parameter n is fixed to $n = 1$. We have studied the case $n = 2$ to see if the process is still critical. In the Figure 4.5 two event series for $n = 1$ and $n = 2$ are shown.

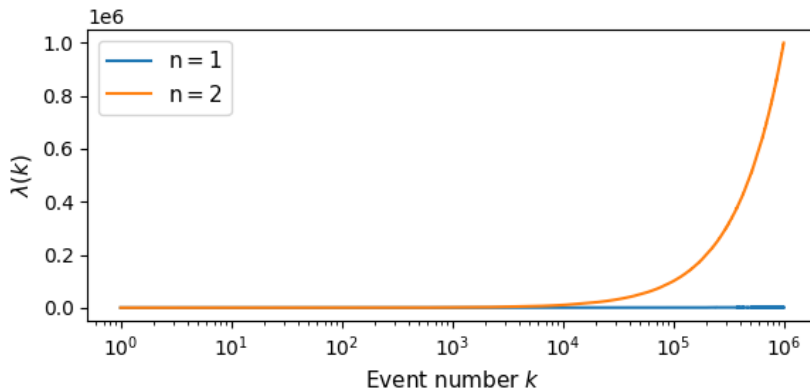


Figure 4.5. Event series for $n = 1$ and $n = 2$.

As presented in the figure above, the rate of the process for $n = 2$ explodes in comparison with the rate for $n = 1$. This is due to the fact that choosing $n = 2$ makes the process supercritical. Similarly to the previous section, the first step is obtaining the phase diagram in order to distinguish the regimes.

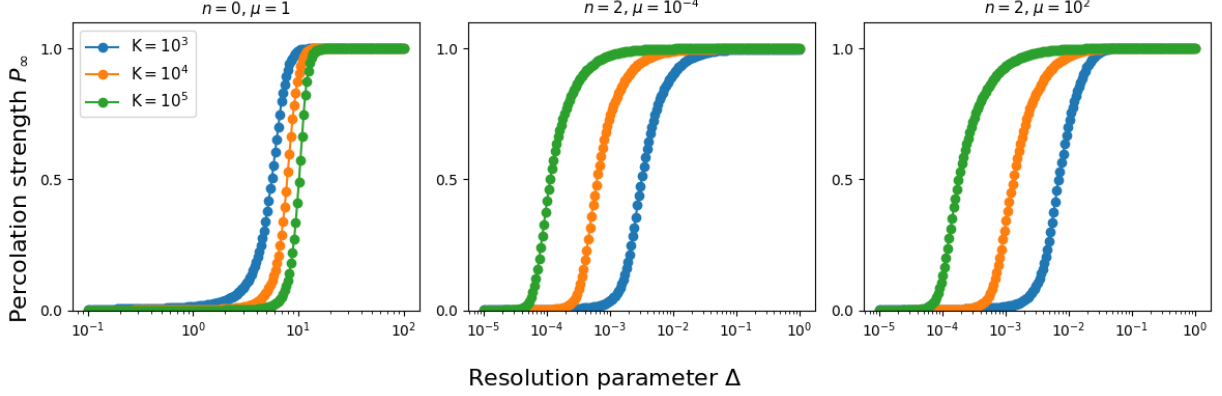


Figure 4.6. Percolation phase diagrams for a Hawkes process with $n = 2$.

In this case, Eqs. 4.2,4.3 are not valid because they were derived for $n = 1$. Therefore, we will obtain this parameter graphically from the phase diagrams shown in Figure 4.6. We will establish Δ^* at the resolution parameter where the percolation strength $P_\infty = 0.5$, consequently, $\Delta^* \approx 10^{-4}$ for both cases. Alike the previous section, in Figure 4.7 the susceptibility is shown.

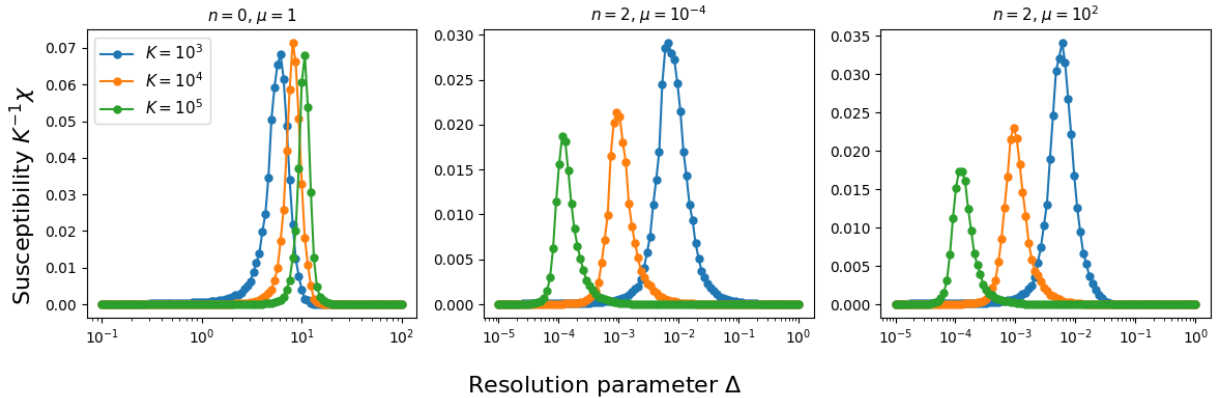


Figure 4.7. Susceptibility χ normalized to the number of events K , for different event number K and taking average values for $R = 1000$ realizations.

As we can recognize from both figures, now we have a single transition for $\mu = 10^{-4}$ and $\mu = 10^2$, in principle corresponds to 1D percolation, ergo, the exponents for the size and duration should be $\alpha = \tau = 2$. Identically to the case of $n = 1$, we have studied the avalanches for $K = 10^5$ events and $R = 1000$ realizations to obtain the histograms. The statistics of the avalanches are shown in Figure 4.8.

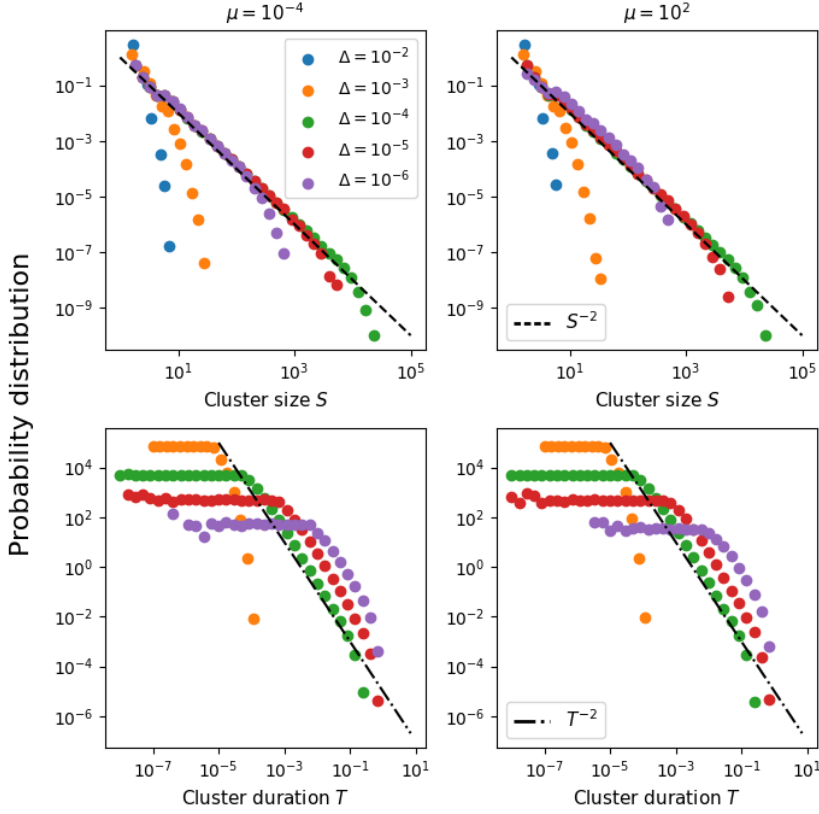


Figure 4.8. Avalanche statistics for a self-exciting Hawkes process with $n = 2$ for $K = 10^5$ events. The histograms have been calculated over $R = 1000$ time series.

avalanches but not caused by criticality as we have seen in the susceptibility diagram, χ only diverges at Δ^* .

As the image shows, we have obtained the exponents $\alpha = \tau = 2$ for both cases, which is compatible with the universality class of 1D percolation. Knowing the time series, like the ones shown in Figure 1.10, after the first event, we find a unique cluster of events caused by the supercriticality. This situation is analogous to the one shown in the case of $n = 1, \mu = 10$ (Figure 1.9) but with a more pronounced effect due to the value of n . Moreover, as happened with $n = 1$, the cutoff of the power-law (caused by the finite size of K) for the cluster duration monotonically shift to higher values as Δ increases. In conclusion, we can also observe percolation phenomena for $n \neq 1$, we also observe power law distributions for the size and duration of the

4.3 Inhibitory and excitatory neurons coupled

To conclude the chapter on results, the results for the case of an excitatory and an inhibitory processes are presented. First of all we will show the results for “pseudo-critical” signals shown in figure 1.13. Both the phase diagrams and avalanche statistics shall be calculated with the event times in general, without distinguishing between excitatory and inhibitory events. Future work could be to study the avalanches for each type of event. As always, the phase diagram and its corresponding susceptibility are shown in Figures 4.9 and 4.10 respectively.

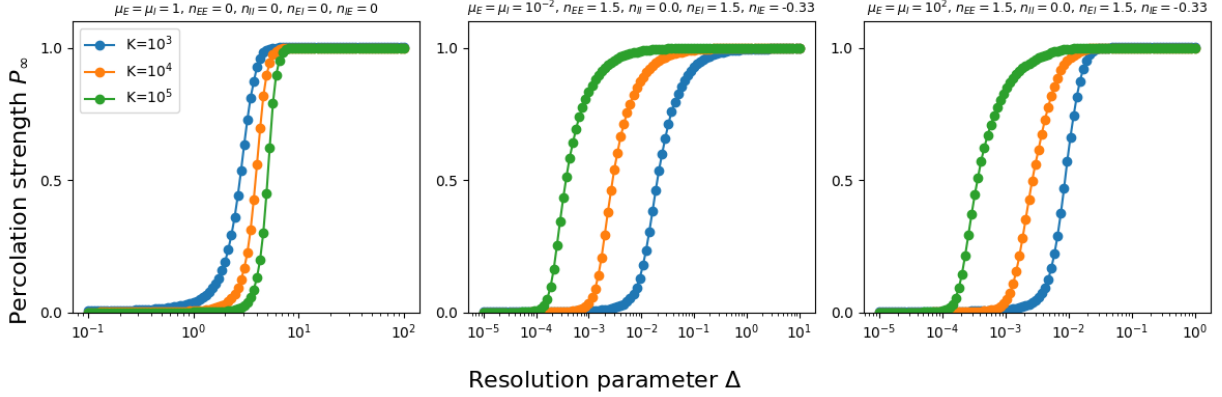


Figure 4.9. Percolation phase diagrams averaged over $R = 1000$ “pseudo-critical” signals of $K = 10^5$ events.

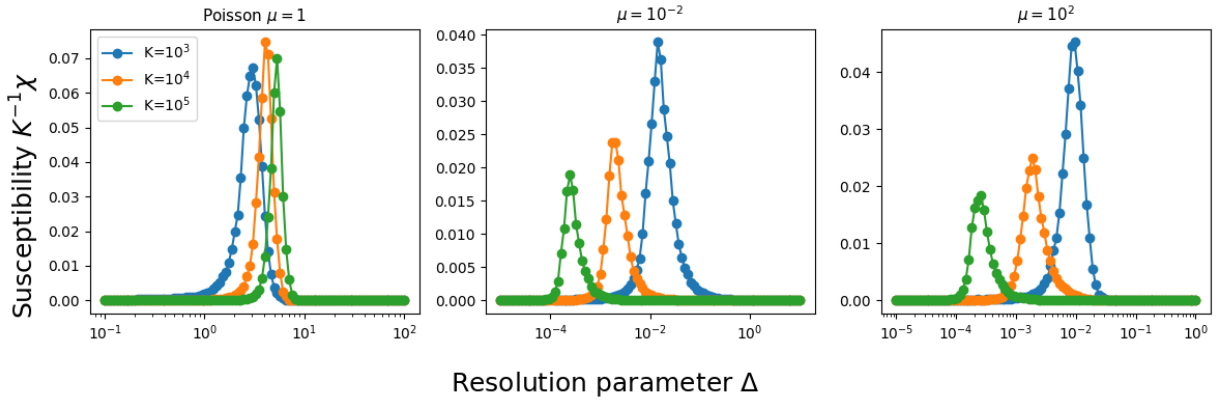


Figure 4.10. Susceptibility χ normalized to the number of events associated with the above the phase diagram.

Both figures show a single transition around $\Delta^* \approx 2 \cdot 10^{-4}$ for 10^5 events, that so far has corresponded with the universality class of 1D percolation, but in this occasion, we have the same situation as in the case of $n = 1$ and $\mu = 10^{-4}$, as illustrated in Figure 4.11.

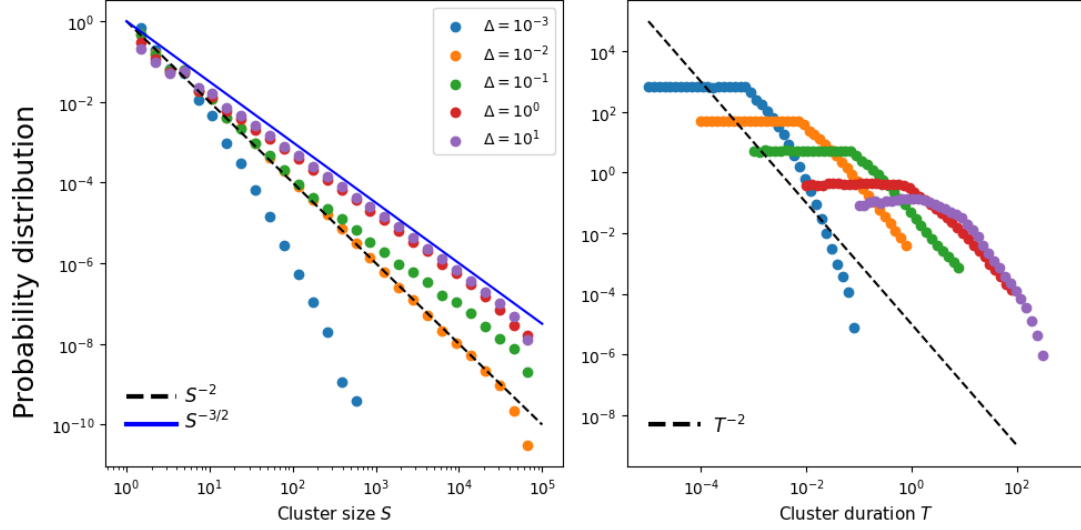


Figure 4.11. Avalanche statistics of $K = 10^5$ events for “pseudo-critical” signals of two coupled Hawkes processes. Histograms have been calculated over $R = 1000$ time series.

In this case, the exponents for the size and duration of the avalanches behave as if there were a double transition in the phase diagram, but without it. On the contrary, for the case of the “controlled” signal shown in Figure 1.14 we do not have this anomaly. The phase diagram and susceptibility are shown in Figures 4.12 and 4.13 respectively.

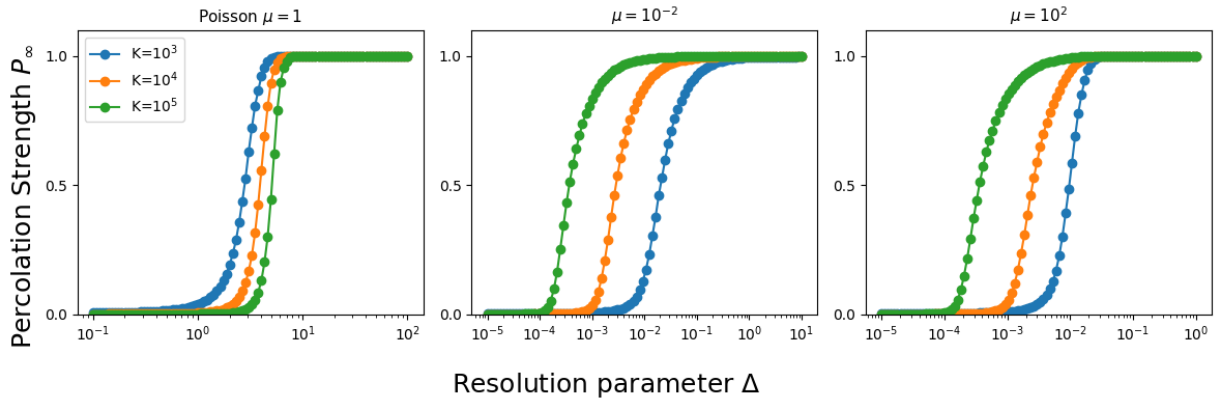


Figure 4.12. Percolation phase diagrams averaged over $R = 1000$ “controlled” signals of $K = 10^5$ events.

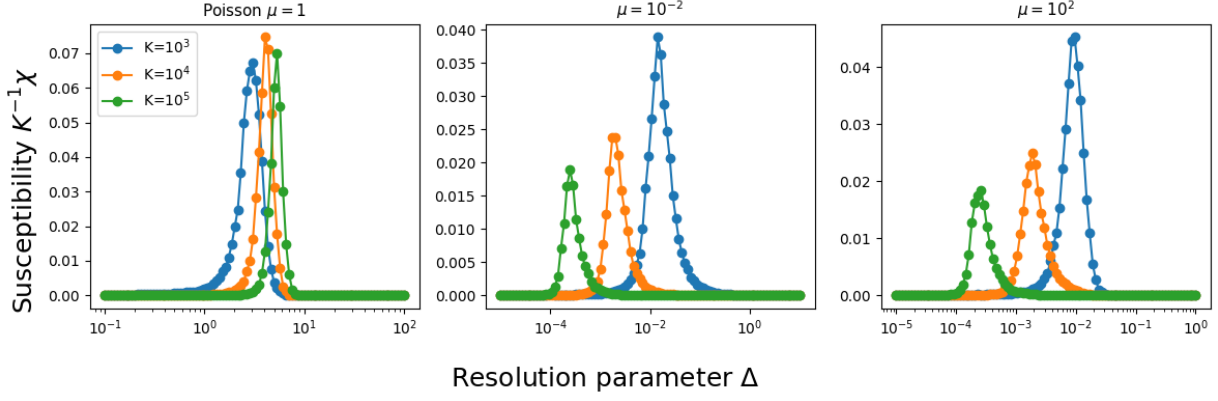


Figure 4.13. Susceptibility χ normalized to K associated with the above the phase diagram.

We note an almost identical behaviour to the one shown in the case of the “pseudo-critical” signals with just a single transition around $\Delta^* \approx 2 \cdot 10^{-4}$ for 10^5 events, agreeing with the universality class of 1D percolation. In this case, as Figure 4.14 indicates, the exponents are indeed $\alpha = \tau = 2$.

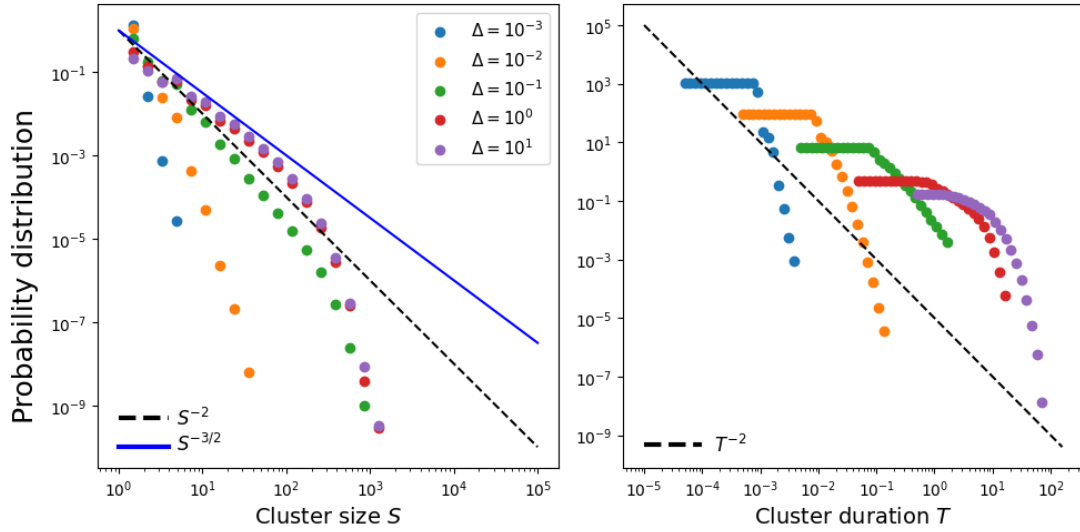


Figure 4.14. Avalanche statistics of $K = 10^5$ events for “controlled” signals of two coupled Hawkes processes. Histograms have been calculated over $R = 1000$ time series.

To conclude the chapter, in Table 4.1 are presented all the exponents obtained for the different configurations studied.

Table 4.1. Power-law exponents for every configuration studied.

	Poisson	n=1		n=2		Coupled processes	
	$\mu = 1$	$\mu = 10^{-4}$	$\mu = 10^2$	$\mu = 10^{-4}$	$\mu = 10^2$	“Pseudo-critical”	“Controlled”
α	2	$2 \xrightarrow{\Delta \uparrow} 3/2$	2	2	2	$2 \xrightarrow{\Delta \uparrow} 3/2$	2
τ	2	2	2	2	2	2	2

Chapter 5

Conclusions

To conclude, this Master's thesis has brought us closer to the comprehension of criticality emerging from Hawkes processes. We have fulfilled the objectives set at the beginning of the project, starting from giving a brief overview of criticality of complex systems, with examples in different fields, such as physics or living systems. After a short introduction to point processes, we also have understood Hawkes processes themselves, how they can be used to model self-exciting events, and how they can be simulated. We have also seen how criticality arises from these processes as long as suitable parameters and time binning are chosen. We have developed computational tools to reproduce the results of the paper by [9] satisfactorily. Furthermore, we also have studied other configurations other than the one presented in the paper, obtaining valuable insights into the system dynamics. Finally, we have begun to explore the coupling of these processes in order to approach a more realistic model of the brain. Further research could be the analysis of the parameter space of two coupled Hawkes processes, the examination of the statistics of excitation and inhibition separately, the study of more processes or the influence of a network structure in the dynamics of the system.

Bibliography

- [1] Miguel A Munoz. “Colloquium: Criticality and dynamical scaling in living systems”. In: *Reviews of Modern Physics* 90.3 (2018), p. 031001.
- [2] Marco Baiesi and Maya Paczuski. “Scale-free networks of earthquakes and aftershocks”. In: *Physical Review E—Statistical, Nonlinear, and Soft Matter Physics* 69.6 (2004), p. 066106.
- [3] Romualdo Pastor-Satorras et al. “Epidemic processes in complex networks”. In: *Reviews of modern physics* 87.3 (2015), pp. 925–979.
- [4] Claudio Castellano, Santo Fortunato, and Vittorio Loreto. “Statistical physics of social dynamics”. In: *Reviews of modern physics* 81.2 (2009), p. 591.
- [5] Sofía Aparicio, Javier Villazón-Terrazas, and Gonzalo Álvarez. “A model for scale-free networks: application to twitter”. In: *Entropy* 17.8 (2015), pp. 5848–5867.
- [6] Albert-László Barabási and Réka Albert. “Emergence of scaling in random networks”. In: *science* 286.5439 (1999), pp. 509–512.
- [7] E. Ising. “Contribution to the theory of ferromagnetism”. In: *Z. Phys* 31.1 (1925), pp. 253–258.
- [8] Jens Wilting and Viola Priesemann. “25 years of criticality in neuroscience—established results, open controversies, novel concepts”. In: *Current opinion in neurobiology* 58 (2019), pp. 105–111.
- [9] Daniele Notarmuzi et al. “Percolation theory of self-exciting temporal processes”. In: *Physical Review E* 103.2 (2021), p. L020302.
- [10] Dietrich Stauffer and Ammon Aharony. *Introduction to percolation theory*. Taylor & Francis, 2018.
- [11] Gerardo Chowell et al. “Mathematical models to characterize early epidemic growth: A review”. In: *Physics of life reviews* 18 (2016), pp. 66–97.
- [12] Sandro Azaele et al. “Statistical mechanics of ecological systems: Neutral theory and beyond”. In: *Reviews of Modern Physics* 88.3 (2016), p. 035003.
- [13] Alan J McKane. *Stochastic Processes*. 2009.
- [14] Kiyoshi Kanazawa and Didier Sornette. “Ubiquitous power law scaling in nonlinear self-excited Hawkes processes”. In: *Physical review letters* 127.18 (2021), p. 188301.
- [15] Angelos Dassios and Hongbiao Zhao. “Exact simulation of Hawkes process with exponentially decaying intensity”. In: (2013).
- [16] Patrick J Laub, Young Lee, and Thomas Taimre. *The elements of Hawkes processes*. Springer, 2021.
- [17] Felipe Yaroslav Kalle Kossio et al. “Growing critical: self-organized criticality in a developing neural system”. In: *Physical review letters* 121.5 (2018), p. 058301.
- [18] Wes McKinney. *Python for data analysis: Data wrangling with Pandas, NumPy, and IPython*. “” O’Reilly Media, Inc.”, 2012.

- [19] Jake VanderPlas. *Python data science handbook: Essential tools for working with data.* ” O’Reilly Media, Inc.”, 2016.
- [20] Travis Oliphant et al. *NumPy*. <https://numpy.org/>. Accessed: 2024-06-21. 2024.
- [21] John D. Hunter et al. *Matplotlib*. <https://matplotlib.org/>. Accessed: 2024-06-21. 2024.
- [22] Adrian Barbu, Song-Chun Zhu, et al. *Monte Carlo Methods*. Vol. 35. Springer, 2020.
- [23] Raúl Toral and Pere Colet. *Stochastic numerical methods: an introduction for students and scientists*. John Wiley & Sons, 2014.
- [24] D Stauffer and C Jayaprakash. “Critical exponents for one-dimensional percolation clusters”. In: *Physics Letters A* 64.5 (1978), pp. 433–434.
- [25] Antonio Rivas Blanco. *TFM*. 2024. URL: <https://github.com/RivasAntonio/TFM>.

Appendix A

Python scripts

REVISAR LOS CÓDIGOS PARA QUE ESTÉN ACTUALIZADOS

CAMBIAR FUNCIONES.PY PARA QUITAR LA GENERATE_SERIES_PERC

AÑADIR FUNCIÓN DE POISSON Y GITHUB EN LA bibliografía Here are the main functions used in the project. The first one is the algorithm used to simulate the inter-event time of a Hawkes process with exponential kernel. The second one is the function for the generation of time series of these Hawkes processes. The third one is the function associated to the calculation of the percolation strength, P_∞ , for the phase diagrams. The fourth one is the function to identify the clusters size and duration distribution. The fifth one is the function to generate the inter-event time of a bivariate Hawkes process with exponential kernel. The last one is the function to generate the time series of the bivariate Hawkes process. Data analysis and plotting functions are not included here, but they can be found in the GitHub repository of the project [25].

Script A.1. Script with the main functions.

```
1 import numpy as np
2
3 def algorithm(rate, mu, n):
4     """
5     Algorithm that computes interevent times and Hawkes intensity for a self-exciting
6     process
7
8     ## Inputs:
9     rate: Previous rate
10    mu: Background intensity
11    n: Weight of the Hawkes process
12
13    ## Outputs: rate x_k, x_k
14    x_k: Inter-event time
15    rate_tk: Intensity at time tk
16    """
17    # 1st step
18    u1 = np.random.uniform()
19    if mu == 0:
20        F1 = np.inf
21    else:
22        F1 = -np.log(u1) / mu
23
24    # 2nd step
25    u2 = np.random.uniform()
```

```

25     if (rate - mu) == 0:
26         G2 = 0
27     else:
28         G2 = 1 + np.log(u2) / (rate - mu)
29
30
31     # 3rd step
32     if G2 <= 0:
33         F2 = np.inf
34     else:
35         F2 = -np.log(G2)
36
37     # 4th step
38     xk = min(F1, F2)
39
40     # 5th step
41     rateTk = (rate - mu) * np.exp(-xk) + n + mu
42     return rateTk, xk
43
44 def generate_series(K, n, mu):
45     """
46     Generates temporal series for K Hawkes processes
47
48     ##Inputs:
49     K: Number of events
50     n: Strength of the Hawkes process
51     mu: Background intensity
52
53     ##Output:
54     times_between_events: time series the inter-event times
55     times: time series the events
56     rate: time series for the intensity
57     """
58     times_between_events = [0]
59     rate = [mu]
60     for _ in range(K):
61         rateTk, xk = algorithm(rate[-1], mu, n)
62         rate.append(rateTk)
63         times_between_events.append(xk)
64     times = np.cumsum(times_between_events)
65     return times_between_events, times, rate
66
67 def calculate_percolation_strength(times_between_events, deltas):
68     """
69     Calculate the percolation strength for a given set of deltas (resolution parameters)
70
71     ## Inputs:
72     times_between_events: time series of interevent times
73     deltas: list of resolution parameters
74
75     ## Output:
76     percolation_strengths: list of percolation strengths
77     """
78
79     percolation_strengths = []
80
81     for delta in deltas:
82         cluster_sizes = []
83         current_cluster_size = 1 # The first event is always a cluster
84
85         for time in times_between_events:
86             if time < delta:

```

```

87         current_cluster_size += 1
88     else:
89         if current_cluster_size > 1: # Only consider clusters with more than one
event
90             cluster_sizes.append(current_cluster_size)
91             current_cluster_size = 1 # The next event is always a cluster
92
93         if current_cluster_size > 1: # Consider the last cluster if it ends at the last
event
94             cluster_sizes.append(current_cluster_size)
95
96         if len(cluster_sizes) != 0: # Check if cluster_sizes is not empty to avoid
errors
97             max_cluster_size = max(cluster_sizes)
98         else:
99             max_cluster_size = 0
100
101         percolation_strengths.append(max_cluster_size / len(times_between_events))
102
103     return percolation_strengths
104
105
106 def identify_clusters(times, delta):
107     """
108     Identifies clusters in a temporal series given a resolution parameter delta
109     Computes the size and duration of clusters
110
111     ## Inputs:
112     times: temporal series
113     delta: resolution parameter
114
115     ## Output:
116     clusters: list of clusters
117     clusters_sizes: list of sizes of clusters
118     clusters_times: list of durations of clusters
119     """
120     clusters = []
121     current_cluster = []
122     for i in range(len(times) - 1):
123         if times[i + 1] - times[i] <= delta:
124             if not current_cluster:
125                 current_cluster.append(times[i])
126                 current_cluster.append(times[i + 1])
127             else:
128                 if current_cluster:
129                     clusters.append(current_cluster)
130                     current_cluster = []
131
132     clusters_sizes = [len(cluster) for cluster in clusters]
133     clusters_times = [cluster[-1] - cluster[0] for cluster in clusters]
134     return clusters, clusters_sizes, clusters_times
135
136 def bivariate_algorithm(rate1, rate2, muE, muI, nEE, nII, nEI, nIE):
137     """
138     Algorithm that computes interevent times and Hawkes intensity for a bivariate Hawkes
process
139
140     #Inputs:
141     rate1: Previous excitation rate
142     rate2: Previous inhibition rate
143     nEE: "Strength" of the autoexcitation process
144     nII: "Strength" of the autoinhibition process

```

```

145 nEI: "Strength" of the excitation to the inhibition
146 nIE: "Strength" of the inhibition to the excitation
147 muE: Background intensity of the excitation
148 muI: Background intensity of the inhibition
149
150
151 """#Output: ratex_k, x_k, reaction (0 for excitatory events and 1 for inhibitory events)
152 """
153 _, xk1 = algorithm(rate1, muE, nEE)
154 _, xk2 = algorithm(rate2, muI, nII)
155
156 xks = [xk1, xk2]
157
158 reaction = np.argmin(xks)
159
160 rate1_tk = 0.
161 rate2_tk = 0.
162
163 if reaction == 0:
164     rate1_tk = (rate1 - muE) * np.exp(-xk1) + nEE + muE
165     rate2_tk = (rate2 - muI) * np.exp(-xk1) + nEI + muI
166 else:
167     rate1_tk = (rate1 - muE) * np.exp(-xk2) + nIE + muE
168     rate2_tk = (rate2 - muI) * np.exp(-xk2) + nII + muI
169
170
171 if rate1_tk <= muE:
172     rate1_tk = muE
173 if rate2_tk <= muI:
174     rate2_tk = muI
175
176 xk = xks[reaction]
177
178 return rate1_tk, rate2_tk, xk, reaction
179
180 def generate_series_bivariate(K, nEE, nII, nEI, nIE, muE, muI):
181     """
182     Generates temporal series for K bivariate Hawkes processes
183
184     ##Inputs:
185     K: Number of events
186     nEE: "Strength" of the autoexcitation process
187     nII: "Strength" of the autoinhibition process
188     nEI: "Strength" of the excitation to the inhibition
189     nIE: "Strength" of the inhibition to the excitation
190     muE: Background intensity of the excitation
191     muI: Background intensity of the inhibition
192
193     ##Output:
194     times_between_events: time series the interevent times
195     times: time series the events
196     rate1: time series for the intensity of process 1 (Excitation)
197     rate2: time series for the intensity of process 2 (Inhibition)
198     reactions: list the event type (0 for excitation. 1 for inhibition)
199     """
200     times_between_events = [0]
201     rate1 = [muE]
202     rate2 = [muI]
203     reactions = []
204     for _ in range(K):
205         rate1_tk, rate2_tk, xk, reaction = bivariate_algorithm(rate1[-1], rate2[-1], muE,
206             muI, nEE, nII, nEI, nIE)

```

```
206         rate1.append(rate1_tk)
207         rate2.append(rate2_tk)
208         reactions.append(reaction)
209         times_between_events.append(xk)
210     times = np.cumsum(times_between_events)
211
212     return times_between_events, times, rate1, rate2, reactions
```